In presenting the dissertation as a partial fulfillment of the requirements for an advanced degree from the Georgia Institute of Technology, I agree that the Library of the Institute shall make it available for inspection and circulation in accordance with its regulations governing materials of this type. I agree that permission to copy from, or to publish from, this dissertation may be granted by the professor under whose direction it was written, or, in his absence, by the Dean of the Graduate Division when such copying or publication is solely for scholarly purposes and does not involve potential financial gain. It is understood that any copying from, or publication of, this dissertation which involves potential financial gain will not be allowed without written permission.

7/25/68

A STUDY OF ION PAIRING IN THE CADMIUM (II) – ETHYLENE bis(OXYETHYLENENITRILO)N,N,N',N' TETRAACETIC ACID – POTASSIUM NITRATE SYSTEM

A THESIS

Presented to

The Faculty of the Division of Graduate

Studies and Research

By

Walter McDonald Shackelford

In Partial Fulfillment

of the Requirements for the Degree

Doctor of Philosophy

in the School of Chemistry

Georgia Institute of Technology

September, 1971

A STUDY OF ION PAIRING IN THE CADMIUM (II) –

ETHYLENE bis(OXYETHYLENENITRILO)N,N,N',N' TETRAACETIC ACID –

POTASSIUM NITRATE SYSTEM

Approved:

Chairman

Date approved by Chairman: 30 Aug 71

ACKNOWLEDGMENTS

I wish to thank my preceptor, Dr. P. E. Sturrock for his guidance, friendship and encouragement in both research work and in the preparation of this manuscript. Dr. H. Flaschka and Dr. J. A. Bertrand are also gratefully thanked for their helpful suggestions concerning the writing of this work.

Additionally, I thank my wife, Bonnie, for her patience.

TABLE OF CONTENTS

TABLE OF CONTENTS (Concluded)

LIST OF TABLES

LIST OF ILLUSTRATIONS

SUMMARY

Ion pair formation has been postulated to explain a number of effects which are evidenced in polarographic studies of the electrical double layer. Previous to this work, however, studies which resulted in the conclusion that ion pairs were present were confined to polarographic means. In the present study, use was made of a potassium-sensitive electrode to determine if ion pairing was an effect only of the double layer or if this phenomenon were present throughout the bulk of the solution. The extent of ion pairing was studied as well as the effects of ion pair formation on the electrode reaction.

Cadmium complexes of ethylene bis(oxyethylenenitrilo)N,N,N',N' tetraacetic acid (EGTA) with a supporting electrolyte of potassium nitrate were studied both polarographically and with the potassium-sensitive electrode to determine the extent of ion pairing between the cadmium-EGTA complexes and potassium ion. pH titrations of EGTA with and without cadmium and potassium present allowed the calculation of acidity constants for the acid and its cadmium and potassium complexes. From these constants the relative distribution of the cadmium complexes at various pH values was calculated.

Although ion pairing showed no noticeable effects upon the acidity of cadmium-EGTA complexes, the ion selective electrode studies gave good evidence for the formation of such pairs. A formation constant of 10 was calculated for the formation of the ion pair $K(CdEGTA)^-$. It was postulated

that the pair is a mixed metal complex.

The polarographic study here was performed utilizing instantaneous d.c. polarography. Data treatment was accomplished through Gierst plots. Results from this study indicated formation of ion pairs in addition to that shown in the ion-selective electrode work. Species such as $K(CdH_2\text{-}EGTA)^+$, $K_2(CdHEGTA)^+$, and $K_2(CdEGTA)$ were proposed to exist in addition to that above.

CHAPTER I

INTRODUCTION

Ion pair formation in aqueous solutions is of interest in polarographic studies involving irreversible electrode reactions because of the change in charge on the electroactive species when paired with an oppositely charged metal ion. Since the charge on the electroactive species in some measure determines its concentration at the reaction plane, the rate of an irreversible electrode reaction will be changed if the charge of the electroactive species is altered. A considerable amount of work has been reported which proposes that ion pairing occurs between a negatively charged electroactive species and an alkali metal ion from the supporting electrolyte. The ion pairing, although it is not considered rate determining, affects the overall rate of the electrode reaction.

In the reduction of copper(II) pyrophosphate (1), extensive ion pairing of the copper(II) pyrophosphate complexes with potassium ion was proposed to account for the unexpected charge that was determined for the reducible species. In that work, a potassium ion-complex species ratio of 2:1 was envisioned for protonated forms of the copper(II) pyrophosphate as well as for the unprotonated forms.

The cadmium-EDTA system has been studied for effects of the supporting electrolyte on the reduction of cadmium-EDTA species (2). Ion pairing mechanisms were proposed and a formation constant of 7.0 was calculated for a potassium-cadmium-EDTA ion pair. However, buffer solutions

were used extensively, and, therefore, the finding of that work is not applicable when the double-layer effects are to be considered with any degree of accuracy.

L. Gierst (3) in a comprehensive study of the double-layer effects on electrode reactions proposed that ion pairing considerably affected the reduction of several species at the electrode. Most of his work was devoted to the study of mechanisms of electrode reactions, and ion pairing figured heavily in some hypotheses.

Studies of ion pairing up to the present have not demonstrated the formation of these species in the bulk of the solution by means of methods other than polarography, since it was postulated that ion pairing was a phenomenon of the double layer only. In the present study, however, use was made of a potassium-selective electrode (glass-membrane) to decide whether or not ion pairing seen in polarographic work was solely taking place within the electrical double layer at an electrode-solution interface.

The system chosed for study consisted of cadmium nitrate, ethylene-bis(oxyethylenenitrilo)N,N,N',N' tetraacetic acid (EGTA*), and potassium nitrate in aqueous solutions. Cadmium and EGTA, in solution, react to form a series of complexes of which, with increasing pH, $Cd(H_2EGTA)$, $Cd(HEGTA)^-$, and $Cd(EGTA)^{2-}$ become predominate. Polarography of the system shows that a decrease in the current follows the increase of $Cd(EGTA)^{2-}$ concentration. Thus, the indication is that this species is not reduc-

*The abbreviation EGTA comes from the name, EthyleneGlycolobis (aminoethylether)N,N,N',N', Tetraacetic Acid, which is no longer in use.

ible. The polarographic waves for a mixture of the complex species appear to be irreversible; therefore, if ion pairing occurs, the rate of the electrode reaction should be affected.

Consideration of ion pairing in this study includes both analysis of polarographic data to elucidate ion pairing effects at the electrical double layer and experimentation employing pH titrations and the ion-selective electrode to determine the extent of potassium binding to EGTA and EGTA complexes of cadmium.

The study of ion pairing phenomena at the electrode double layer was made using instantaneous d.c. polarography. Potassium nitrate was employed in various concentrations (0.05 F, 0.1 F, 0.5 F, and 1.0 F). Since the potassium nitrate concentration was at least 25 times that of the complex species, it could be considered to determine all double layer characteristics of the system. A study was undertaken to find out whether adsorption of either reactants or products at the electrode occurred. Adsorption of the nitrate ion was compensated for by the use of the data reported by Payne (4) for the potassium nitrate system. To characterize the double layer for this system, use was made of the Gouy-Chapman theory as modified by Stern (5).

Since the pH of the solution determines the types of cadmium complexes present, studies were performed at various pH values (2.50, 3.00, 3.50, 4.00, and 4.50). The reduction of $Cd(EGTA)^{2-}$ is so irreversible that above pH 4.50, where this species is essentially the only one present, no reduction wave is observed at all. In Chapter V, a description of the polarography of the system is given with relation to the distribution of complex species.

The method of Gierst was used whenever possible to investigate the effects of various parameters on the polarization curve. These parameters are: specific adsorption, double-layer, pH, ion-pair formation, and electrochemical kinetics.

In order to establish the composition of the bulk of the solutions, pH titrations and measurements with the ion-sensitive electrode were used. The type and concentrations of various complexes were established, the degree of ion pairing calculated, and the relative distribution of species found.

The acidity constants of protonated EGTA complexes of cadmium and of potassium have been computed as well as the formation constants of the various complex species. These data are given in Chapter IV.

CHAPTER II

EXPERIMENTAL METHODS

Use of the Ion-Selective Electrode

Theory

For many years measurement of hydrogen ion activity has been accomplished with the use of the glass electrode. Early experiments with glass membrane electrodes showed that the potential difference across the membrane could be predicted by a Nernst-type equation (6),

$$V = \text{const.} + \frac{RT}{nF} \ln a_{H}^{+} \qquad (2\text{-}1)$$

where V is the potential in volts, a_{H}^{+} is the activity of the hydrogen ion, and R, T, and F are the gas constant, absolute temperature, and Faraday's constant, respectively; n is the number of electrons involved in the electrochemical reaction, and has a value of one in this case.

Non-adherence to this equation becomes evident, however, at very high ($pH \leq 2$) and at very low ($pH \geq 11$) hydrogen ion activities. It was noted that at high pH with alkali metal ions present potentiometric measurements using the glass electrode gave a lower pH than was correct for the solution. Further studies indicated that the amount of alkali metal ion present determined the extent of this so-called alkaline error (7). Subsequent investigations showed that glasses with high boron oxide content were nearly as sensitive to sodium ion as to hydrogen ion (8).

G. Eisenman (9), in a systematic study of simple glasses containing only sodium oxide, aluminum oxide, and silica, has shown that not only sodium ions, but also other alkali metal ions, e.g. lithium, potassium, and rubidium, cause a reproducible response.

The choice of the glass composition for a particular electrode is dependent upon the extent of the alkaline error desired. For electrodes sensitive to alkali metal ions, fusion of silica and the oxides of a trivalent and monovalent metal is performed to make a three-dimensional structure in which the only significantly mobile species is the monovalent cation. The usual ion-selective electrode consists of a thin glass bulb of the desired composition filled with a 1 F solution of the chloride of the metal of interest. A silver-silver chloride reference electrode is suspended in this solution and the whole system is then sealed (10).

When coupled with a suitable external reference electrode the potential due to the difference of concentration of alkali metal ion between the internal reference solution and the sample solution across the glass membrane may be expressed by the relation

$$V = \frac{RT}{F} \ln \frac{a_i}{a_j} \qquad (2\text{-}2)$$

where a_j is the known activity of the metal ion in the bulb and a_i is the activity of this ion in the sample solution (11).

If more than one alkali metal is present, the electrode response depends upon the summed contributions of each cation so that

$$V = \frac{RT}{F} \ln \sum_{i=1}^{n} \frac{p_i a_i}{p_1 a_1} \qquad (2\text{-}3)$$

where p_i and p_1 are the permeabilities of the i^{th} ion and the cation in the bulb, respectively, and a_i and a_1 are their respective activities (12). It should be noted here that at pH $\leqq$ 5 all cation-sensitive glasses are predominantly sensitive toward hydrogen ion and that none of the glass membranes are especially selective among lithium, sodium, and potassium ions. Thus, operation in media containing other than fixed ratios of alkali metal ions is not very satisfactory and operation in solutions of pH $<$ 4 is unfeasible.

In a cation exchange membrane such as glass, the permeability ratio, $\frac{P_i}{P_j}$, can be expressed in terms of the ion exchange equilibrium constant, k, and the mobility ratio, $\frac{U_i}{U_j}$,

$$\frac{P_i}{P_j} = k \frac{U_i}{U_j} \qquad (2\text{-}4)$$

This means that both diffusion and boundary processes are involved in the origin of the potential of the glass electrode as exhibited by

$$V = V_B + V_D + V_{B'} \qquad (2\text{-}5)$$

where V_B is the potential drop across the interface between the reference solution and the glass membrane, V_D is due to diffusion in the glass, and

V_B, is due to the potential drop across the interface between the unknown sample solution and the glass membrane (13). This relation is represented in Figure 1.

Experimental Technique

A Beckman Research pH meter (model 1019) coupled with a Beckman 39137 Cation Electrode and a Fisher "Dri-Pak" saturated calomel electrode was used for all potentiometric measurements. For pH measurements, a Beckman 41263 glass electrode was used instead of the 39137 electrode. Since pH measurements were taken concurrently, the cell was first purged with dry nitrogen to remove carbon dioxide and then blanketed with dry nitrogen. Temperature was kept constant at 25° ± 0.2°C by means of a thermostated water bath.

Calibration plots were established both before and after each run since the ion-selective electrode response changes with time. There was practically no variation during the course of one day, but over longer periods of time small changes in the response toward standard solutions were noted.

pH Titrations

Theory

If an acid can be titrated in the presence of an excess of metal ion without precipitate formation, it is possible to study the complexation of the metal ion with the acid *via* the pH lowering. As long as the inflections at the various equivalence points remain evident when a proton is added to or removed from the molecule, the calculations of the forma-

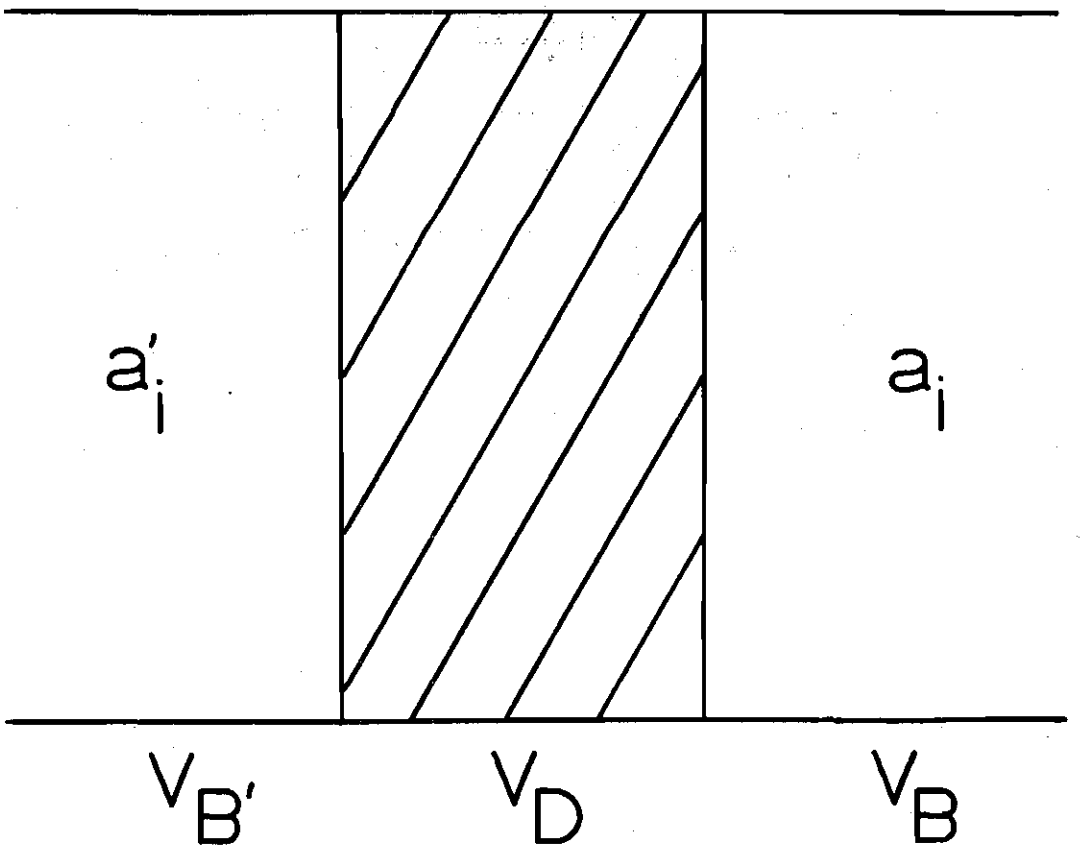

Figure 1. Origin of the Potential of the Glass Electrode

tion constants of the complexes are relatively straight forward. In this case each ligand molecule gains or loses protons in a stepwise manner even though the ligand molecule may also be bound to a metal ion.

For a polyprotic acid such as H_4EGTA the general equation for the stepwise loss of protons is

$$H_nEGTA^{(4-n)-} \rightleftarrows H_{n-1}EGTA^{(5-n)-} + H^+ \tag{2-6}$$

and the corresponding mixed acidity constant is

$$K_{4-n} = \frac{a_{H^+}\left[H_{n-1}EGTA^{(5-n)-}\right]}{\left[H_nEGTA^{(4-n)-}\right]} \tag{2-7}$$

For formation of a complex of EGTA with a monovalent metal ion the general equation is

$$M^+ + H_nEGTA^{(4-n)-} \rightleftarrows M(H_nEGTA)^{(3-n)-} \tag{2-8}$$

and the corresponding formation constant, $K_{MH_nL}^{H_nL}$, is

$$K_{MH_nL}^{H_nL} = \frac{\left[M(H_nEGTA)^{(3-n)-}\right]}{\left[M^+\right]\left[H_nEGTA^{(4-n)-}\right]} \tag{2-9}$$

The acidity constant for the metal complex has been expressed (14) as

$$K'_{(4-n)} = \frac{a_{H^+}\left[M(H_{n-1}EGTA)^{(2-n)-}\right]}{\left[M(H_nEGTA)^{(3-n)-}\right]} \qquad (2\text{-}10)$$

Substitution of Equations (2-7) and (2-9) into Equation (2-10) results in

$$K'_{(4-n)} = \frac{a_{H^+}\left(\left[H_{n-1}EGTA^{(3-n)-}\right] + \left[M(H_{n-1}EGTA)^{(2-n)-}\right]\right)}{\left[H_nEGTA^{(4-n)-}\right]} \qquad (2\text{-}11)$$

which was derived by Watters, et al. (15) for the pyrophosphate system.

Experimental Technique

All titrations were performed in a thermostated water bath at 25° ± 0.2°C. A Beckman 41263 glass electrode and a Fisher "Dri-Pak" saturated calomel electrode were used for pH measurements. All measurements were taken with a Beckman Research pH meter. Each sample was purged with dry nitrogen and then blanketed with the nitrogen.

Polarography

Theory

Irreversibility. Oxidizable or reducible species may be analyzed both qualitatively and quantitatively in solution via the reaction of the

species at a polarized electrode. The particular species in solution has a characteristic half-wave potential--that potential at which the current is one half its diffusion-limited value--and the current produced is proportional to its concentration. If the reaction rate of the species at the electrode is limited by diffusion, the process is said to be reversible. If the current is not limited by diffusion alone, the reduction or oxidation is said to be irreversible. In the case of the cadmium-EGTA system the reaction at the electrode is irreversible in the context of the above statements.

For an irreversible system the equation (16) for the current at some instant in the life of the mercury drop is,

$$i = nFAC\left(\frac{7D}{3\pi t}\right)^{1/2}\left[1 + \left(\frac{D}{D'}\right)^{1/2} \exp\{nf\,(E - E_s\}\right]^{-1} \Gamma_1(\lambda) \qquad (2\text{-}12)$$

where C is the concentration of the reactant in the bulk of the solution, D and D' are the diffusion coefficients of reactant and product, respectively, E is the instantaneous potential, and E_s is the standard potential for the electrochemical reaction. A is the electrode area, t is the time in the drop life, and f is the quotient $\frac{F}{RT}$. Also, in this equation

$$\lambda = k_a^s\left(\frac{t}{D}\right)^{1/2} \exp\{-\alpha nf\,(E - E_s)\}\left(1 + \left(\frac{D}{D'}\right)^{1/2} \exp\{nf(E - E_s)\}\right) \qquad (2\text{-}13)$$

where k_a^s is the standard apparent heterogeneous rate constant for the electrode reaction in either direction at the potential E_s and α is the cathodic transfer coefficient.

By letting x equal the ratio of current at any potential to the diffusion current then

$$x = \left[1 + \left(\frac{D}{D'}\right)^{1/2} \exp\{nf(E - E_s)\}\right]^{-1} \tag{2-14}$$

or

$$x = \Gamma_1(\lambda) = \Gamma_1\left(k_a^s \left(\frac{t}{D}\right)^{1/2} \exp\{-\alpha nf\,(E - E_s)\}\right) \tag{2-15}$$

It has been shown (17) that, empirically,

$$\Gamma_1(\lambda) = \frac{1}{1.35}\left[\frac{2x(3 - x)}{5(1 - x)}\right] \tag{2-16}$$

Thus,

$$\frac{2x(3 - x)}{5(1 - x)} = 1.35 \left(\frac{t}{D}\right)^{1/2} k_a^s \exp\left[-\alpha nf\,(E - E_s)\right] \tag{2-17}$$

Since no double-layer considerations are taken into account, k_a^s is the standard apparent heterogeneous rate constant and is related to the heterogeneous rate, constant, k, at any potential by

$$k = k_a^s \exp\left[-\alpha nf\,(E - E_s)\right] \tag{2-18}$$

Thus, for calculation of the heterogeneous rate constant

$$k = \frac{1}{1.35}\left[\frac{2x(3 - x)}{5(1 - x)}\right]\left(\frac{D}{t}\right)^{1/2} \qquad (2\text{-}19)$$

is used. The correction of k for double-layer effects will be discussed later in Chapter V.

At the half-wave potential

$$E_{1/2} = E_s + \frac{1}{\alpha nf} \ln\left[1.35\left(\frac{t}{D}\right)^{1/2}\right] \qquad (2\text{-}20)$$

thus, at 25°C,

$$\frac{0.0591}{\alpha n} \log\left[\frac{2x(3 - x)}{5(1 - x)}\right] = E_{1/2} - E \qquad (2\text{-}21)$$

From a plot of $\log\left[\frac{2x(3 - x)}{5(1 - x)}\right]$ versus -E numerical values for both the transfer coefficient and the half-wave potential can be obtained.

Double-layer Effects. When an electrode is totally or partially polarized, two layers of ions are attracted to it. These two layers, the inner and outer Helmholz planes, are depicted in Figure 2. The inner Helmholz plane, x_i, constitutes the plane of closest approach for non-hydrated ions while the outer Helmholz plane, x_j, correspondingly is composed of hydrated ions. The inner and outer Helmholz layers compose the compact double layer. The region extending from the outer Helmholz plane to the bulk of the solution is the diffuse double layer. The relationship between potential and the distance from the electrode is shown in Figure 2.

The total potential drop between the electrode surface and the bulk of the solution can be measured readily. For convenience, potential is

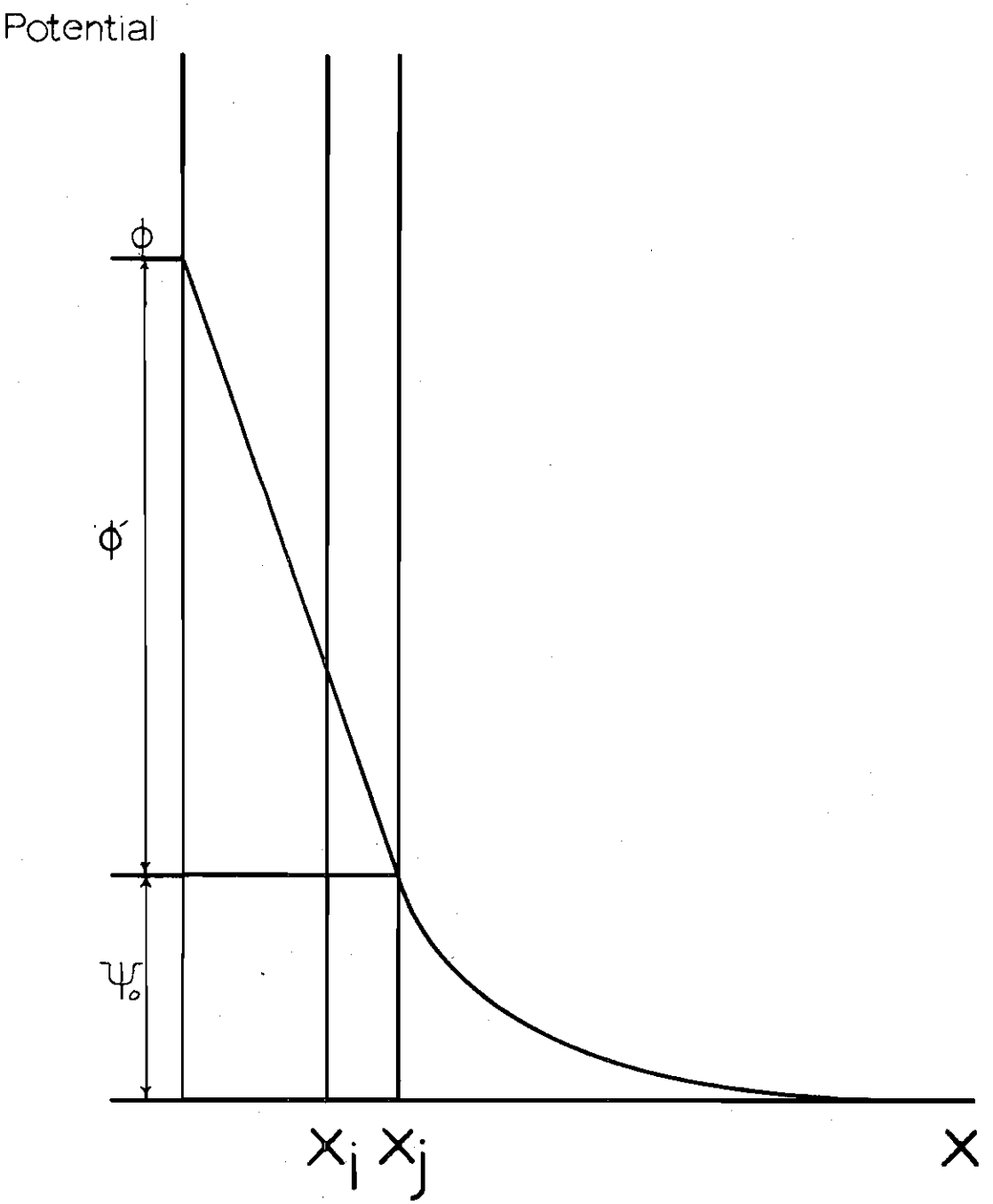

Figure 2. The Relation of Potential to the Distance from the Surface of the Electrode

usually expressed as the rational potential, Φ, i.e. the potential measured with reference to the point of zero charge (PZC). At the PZC $\Phi = 0$ and at any potential

$$\Phi = \psi_o + \Phi' \tag{2-22}$$

where Φ' is the potential drop between the electrode surface and the outer Helmholz plane and ψ_o is the potential drop between the outer Helmholz plane and the bulk of the solution. Since electrode reactions normally are believed to take place at the outer Helmholz plane, Φ', may be considered to be the driving force for the reaction. It will be shown, however, that ψ_o is also a factor.

At the PZC the electrode is not charged and the surface tension at the solution-electrode interface is at its maximum (the electrocapillary maximum). The charge on the electrode is given by the Lippmann equation (17)

$$q = -\frac{d\gamma}{dE} \tag{2-23}$$

where q is the charge on the electrode per unit area, γ is the interfacial surface tension, and E is the potential of the electrode. Calculation of the electrocapillary maximum may be accomplished <u>via</u> drop-time potential plots.

The array of charges surrounding the oppositely charged electrode depends upon both the predominate electrolyte present and the dielectric

constant of the solvent. The physical significance of these two sets of opposite charges is that of a capacitor with its capacitance defined as

$$C_i = - \frac{Q}{\Phi} \tag{2-24}$$

where C_i is called the integral capacitance and Q is the charge on the electrode. The integral capacitance is not easily measurable directly.

The differential capacitance, C_d, is defined by

$$C_d = - \frac{dQ}{dE} \tag{2-25}$$

where E is any potential. The differential capacitance varies with charge for a given potential step and thus can be measured provided dE is not larger than a few millivolts (18).

It can be seen that the differentiation of the interfacial surface tension versus potential curve yields the charge on the electrode. A second differentiation of $\frac{d\gamma}{dE}$ with respect to E is the expression for the differential capacitance. Conversely, q and γ may be obtained by single and double integration, respectively, of Equation (2-25). The integral capacitance may be calculated from Equation (2-24) provided the potential at the PZC is known.

In Stern's modification of the Gouy-Chapman theory (5) ions are considered to have finite size and to approach the electrode only to a certain distance (the plane of closest approach). This modification allows good calculation of ψ_o if no specific adsorption occurs. The equation for the calculation of ψ_o is

$$\psi_o = \left(\frac{2}{fz}\right) \sinh^{-1}\left(\frac{q}{\partial A}\right) \qquad (2\text{-}26)$$

where

$$A = \left(\frac{RT\epsilon C_s}{2\pi}\right)^{1/2}$$

Here ϵ is the dielectric constant, C_s is the concentration of supporting electrolyte and z is the effective charge on the supporting electrolyte. For 1 - 1 electrolytes Equation (2-26) reduces to

$$\psi_o = \frac{2}{38.935} \sinh^{-1}\left(\frac{q}{11.74\ C_s^{1/2}}\right) \qquad (2\text{-}27)$$

The Gierst Plot. In irreversible electrode reactions the rate determining step can be the electrode reaction, a chemical reaction preceding the electrode reaction, or a combination of these two. The rate of the electrode reaction is thus profoundly dependent upon the electrical double layer.

It was stated earlier that Φ' is the driving force of the reaction. Since Φ' is dependent upon ψ_o at constant Φ, the increase of ψ_o for constant Φ should have a noticeable effect upon the reaction rate. If Φ approaches 0.7, ψ_o can readily be greater than 100 mv for salt concentrations of 0.1 F or less. Also, as Gierst has shown (3), the ψ_o potential markedly affects the surface concentration of the reactants. At the plane of closest approach the actual reactant concentration, $[A]_o$, is related to the expected reactant concentration, [A]*, by

$$[A]_o = [A]^* \exp(-zf\psi_o) \tag{2-28}$$

The concentration, $[A]^*$, depends only upon mass transfer considerations; thus, it may be considered practically constant over a wide range of supporting electrolyte concentrations. Therefore, as ψ_o changes, the actual concentration of reactant at the plane of closest approach changes also.

Frumkin (19) has shown that in the presence of double-layer effects the true rate of the electrode reaction, V^o is related to the observed rate, V^*, by

$$V^* = V^o [\exp(-\alpha n f \Phi')] \exp(-zf\psi_o) \tag{2-29}$$

or, in $\log_{10}$ form at 25°C

$$0.0591 \log V^* = 0.0591 \log V^o - \alpha n \Phi' - z\Phi_o \tag{2-30}$$

where n is the number of electrons involved in the electrode reaction and

$$V^* = \frac{1}{1.35}\left[\frac{2x(3 - x)}{5(1 - x)}\right]\left(\frac{D}{t}\right)^{1/2} \tag{2.31}$$

L. Gierst (3) devised a graphical procedure for the evaluation of the factors in the Frumkin equation. Since it can be seen that

$$V^* = F(\Phi)$$

a plot of 0.0591 log V^* versus ψ_o at constant Φ' gives information about z and a plot of 0.0591 log V^* versus Φ' at constant ψ_o gives information about αn.

Generally, these evaluations are carried out in the following manner. A plot of 0.0591 log V^* versus Φ is made for different supporting electrolyte concentrations. On the same graph a plot of ψ_o versus Φ is made for the same supporting electrolyte concentrations on the same scale and below the previous plots. Drawing of constant Φ' and constant ψ_o lines allows a separation of the effects of each and the determination of αn and z. The value of V^o is found as the zero intercept of the line 0.0591 log $V^* = F(\Phi')$.

Experimental Technique

Polarograms were taken using a three electrode cell and a polarograph designed and built in this department. A solenoid system was used for drop detachment to insure uniformity of drop size. Measurements were made at the end of the drop life through the use of a trigger sampling device to insure reproducible sampling. Potentials and currents were read from a digital display accessory to the polarograph. All polarograms were run at 25° ± 0.2°C. Temperature was kept constant by means of a thermostated water bath and the solutions were purged and then blanketed with dry nitrogen.

CHAPTER III

EQUIPMENT, INSTRUMENTATION, AND CHEMICALS

Electrodes and Cells

Ion-selective Electrode and pH Titrations

The ion-selective electrode studies were performed utilizing a Beckman 39137 Cation Electrode, a Fisher "Dri-Pak" saturated calomel electrode (SCE), and a Beckman Research pH meter.

The cation electrode required considerable care in aging and handling to insure reproducible response. When new, the cation electrode was found to have a permeability ratio of 2:1 for potassium over sodium, but with proper aging this ratio increased to about 20:1. The permeability ratio of hydrogen ion to potassium was not calculated but appeared to be greater than 100:1. Thus, in solutions of 10^{-3} F potassium nitrate the lowest pH which could be tolerated was 5.0.

In order to achieve maximum response and reproducibility, the electrode was aged for about two weeks by soaking it in alkaline solutions of 0.1 F potassium nitrate. Although the cation electrode may be used successfully after as little as 24 hours aging, drift in response over a period of a few hours is noticeable after this short aging time.

Since tetramethylammonium hydroxide (TMAOH) was used as the titrant in the ion-selective electrode study, the interference of TMAOH in the cation electrode response to potassium had to be considered. It was found that TMAOH caused no interference in the measurement of potassium ion

concentration in solutions containing TMAOH-potassium nitrate ratios up to 50:1.

The cation electrode was utilized *via* a standard calibration plot of potassium ion concentration versus potential. It was noted for the concentration range of 10^{-2} - 10^{-3} *F* in potassium ion, that plotting of either concentration or activity versus potential gave straight line plots with identical slopes of 59 mv. A typical calibration plot is shown in Figure 3.

It was found that the history of the electrode greatly influenced its response. If the cation electrode were exposed to solutions of pH $\leq$ 4.0, response was not reproducible until treatment in alkaline solution for several hours was accomplished.

For all pH work a Beckman 41263 glass electrode was used in addition to the above mentioned apparatus. No inordinate problems were found with either the glass electrode or the SCE which were employed. Electrode junction potentials were calculated for the SCE for solutions of varying potassium nitrate concentrations, but the highest of the potentials was only 0.6 mv. Thus, electrode junction potentials were ignored.

The cell for both pH and ion-selective electrode work consisted of a 100 ml Berzelius beaker which was stoppered with a No. 10 rubber stopper. Holes were drilled in the stopper to accommodate the glass electrode, the SCE, the cation electrode, and a fritted glass deaerator. The temperature of the cell was maintained at 25° ± 0.2°C utilizing a thermostated water bath. The solution was freed of dissolved oxygen and carbon dioxide by purging with nitrogen for approximately 15 minutes before

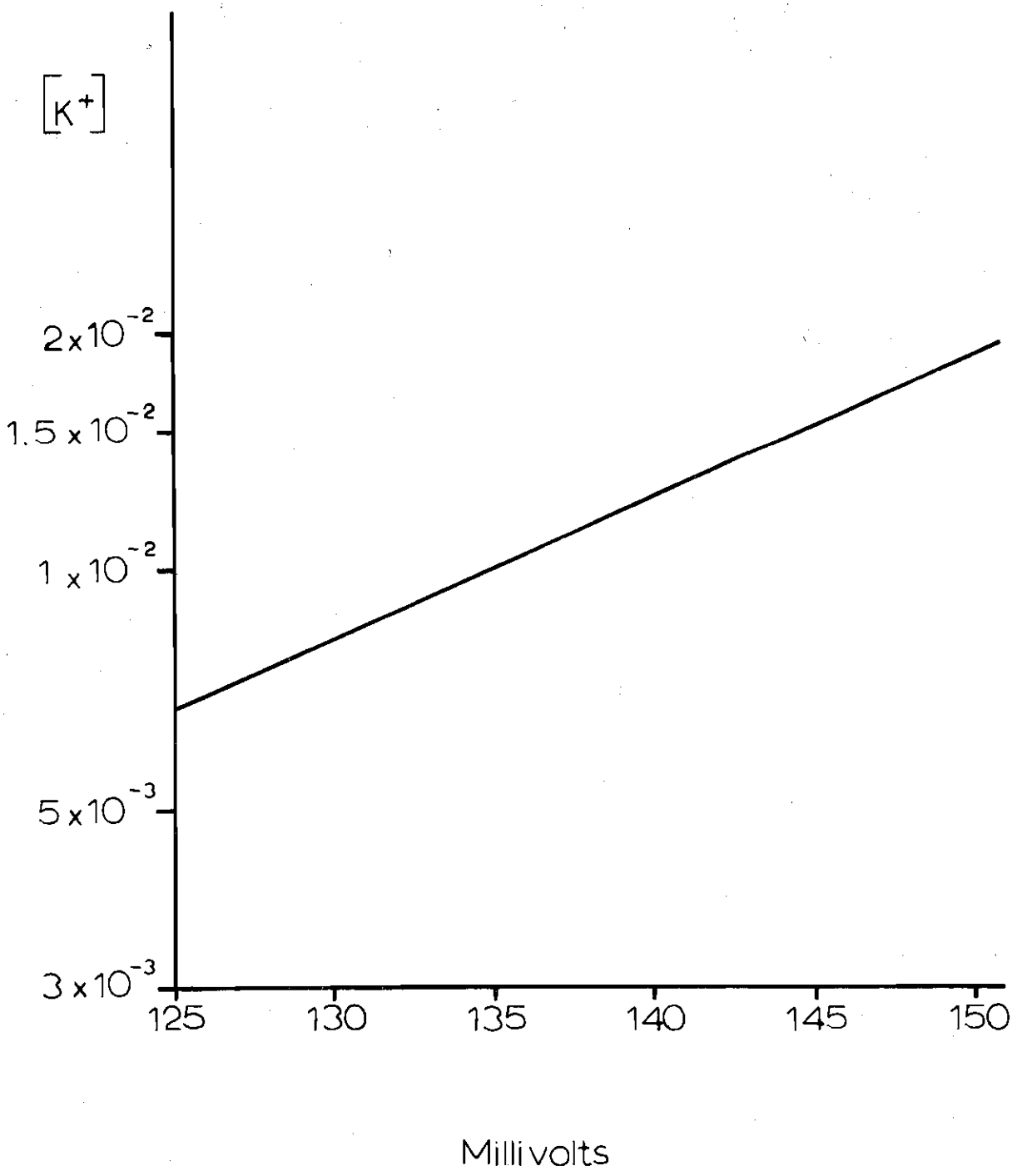

Figure 3. Typical Calibration Plot for the Ion-Selective Electrode

titrating. During the titration the deaerator was only removed from the solution while actually taking a reading. The cation electrode was introduced to the solution only after the pH became greater than 4.0.

Polarography

All polarographic work was done with mercury electrodes. A dropping mercury electrode and a dropping cadmium amalgam electrode were employed.

The dropping mercury electrode was constructed of 6-mm Pyrex glass tubing, a Pyrex reservoir and Tygon tubing which connected the reservoir to the glass tubing. The glass tubing was affixed to a meter stick so that the mercury head could be measured. Two cm from the bottom of the glass tubing a platinum wire was introduced through one wall of the tubing and sealed for connection to the polarograph. One half of a Sargent 2-4 second polarographic capillary was affixed to the bottom of the glass tubing by means of a 5-cm section of hard neoprene tubing. To prevent clogging, the capillary was rinsed with distilled water prior to interruption of the mercury flow and was maintained in air between experiments.

The dropping cadmium amalgam electrode was constructed of a 150-ml amalgam reservoir atop a jacketed glass column of about 20 cm length. Below the jacket a 2-mm stopcock, a through-glass platinum electrical connection and a standard external 10/30 glass joint were included. One half of a Sargent 2-4 second capillary was sealed with Varno cement into a 1-cm glass tubing which had a diameter slightly larger than the capillary. The glass tubing was fused to a standard internal 10/30 glass joint. This arrangement allowed replacement of the capillary without

draining the entire supply of amalgam.

To determine the flowrate of the dropping mercury electrode, a time consuming but simple method was applied. Two hundred drops of mercury were collected at a potential close to the PZC in a solution representative of those used in polarographic studies and the elapsed time was measured. The solution and the resultant mercury pool were separated by decantation and then the mercury was dried with reagent grade acetone and weighed. The flowrate, M, in grams per second, was found from the equation

$$M = \frac{w}{t} \qquad (3\text{-}1)$$

where w is the weight of mercury collected in grams and t is the time. Negligible contact area was assumed for the Sargent capillaries.

The cell consisted of a 100-ml Berzelius beaker stoppered with a No. 10 rubber stopper. The stopper was drilled to accommodate a glass electrode, a SCE, the dropping mercury electrode, a counter electrode consisting of a platinum wire, and fritted glass deaerator. The temperature of the cell was maintained at 25° ± 0.2°C by means of a thermostated water bath.

Polarographic and pH data could be collected concurrently by switching the leads to the SCE. One lead was connected to the pH meter and the other lead was connected to the polarograph. Simultaneous determination of pH and polarographic data was not possible due to the difference in impedance of the two instruments.

Instrumentation

Controlled Potential Polarograph

For all polarographic work, an instrument, which was designed and built in the electronics shop of the School of Chemistry, was used. The instrument has both polarographic and coulometric capabilities. The instrument contains a potentiostat and a current measuring section for performing polarographic functions.

In Figure 4 the basic circuit of the instrument is shown. The cell is a three electrode cell with test electrode, T, counter electrode, C, and reference electrode, R. The potentiostat controls the electrode potential via continuous summation of all the currents received at the summing point, S. The difference in potential between the test electrode and the reference electrode appears at the output of the voltage follower, VF. Regulation of the electrode potential is then achieved by passing current through the cell at the counter electrode. Since essentially no current can pass through the reference electrode-voltage follower combination, virtually all cell current must pass through the test electrode, which is connected to the current follower, CF, to produce a voltage proportional to the cell current.

The integrator provides a voltage ramp for sweeping over any desired potential range. A control to set the initial potential is also available.

Time Delay Generator and Solenoid

Also built in the electronics shop was a chronopotentiometer similar to one designed by Sturrock (20). Although chronopotentiometry was

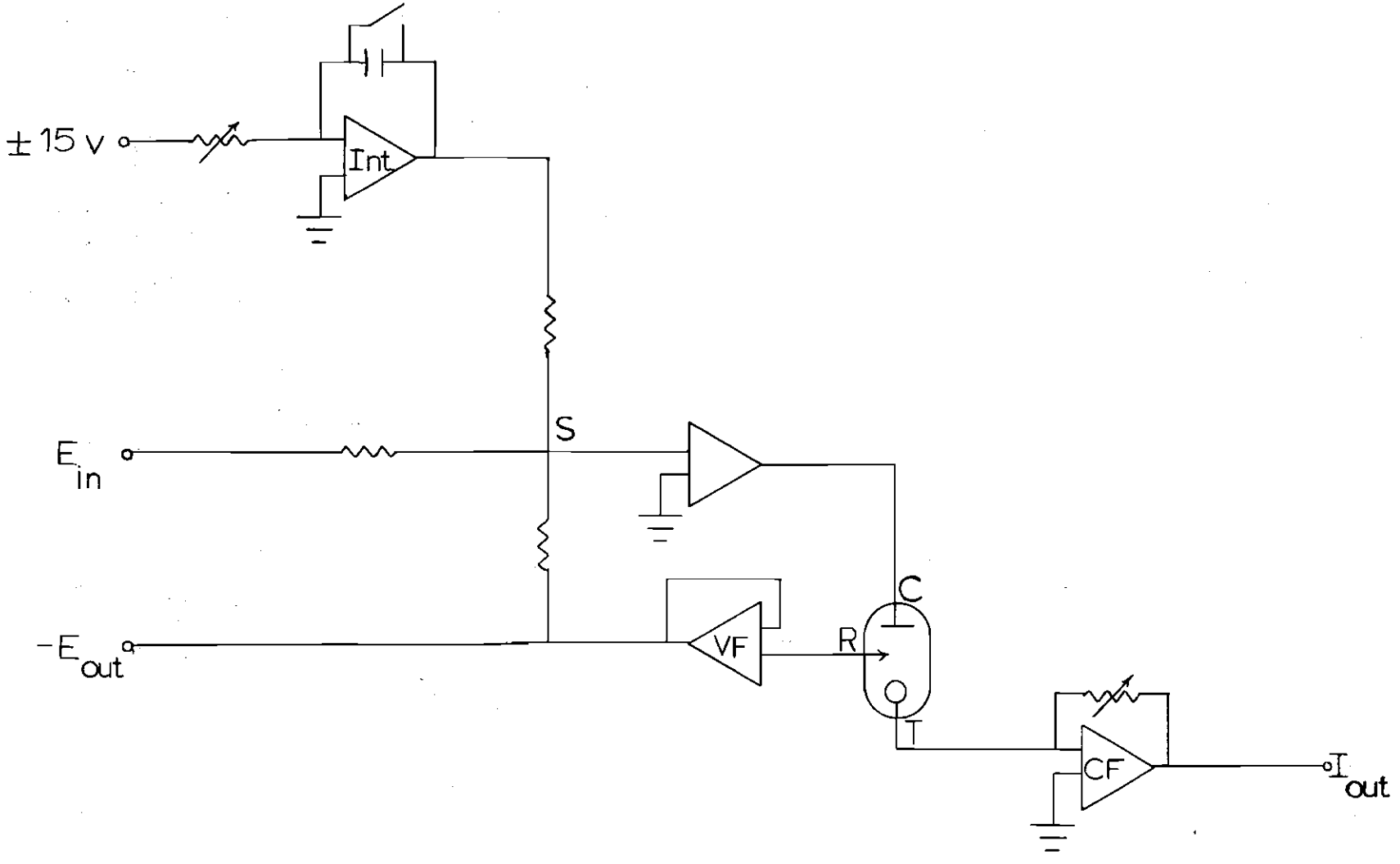

Figure 4. Diagram of the Controlled Potential Polarograph

not a method applied in this research, two functions of the chronopotentiometer were used: the solenoid system and the time delay circuit. The solenoid system consists of a solenoid-actuated plunger with a cycle time regulated by an RC network with a large time constant. For a given setting on the instrument the solenoid is triggered at a constant time interval, dislodging the mercury drop by means of a slight tap on the capillary. The trigger for the solenoid also pulses a monostable oscillator which has an RC constant that may be set for a desired time delay. The pulse from the monostable oscillator then opens a gate to allow sampling of the polarographic current.

Digital Display Accessory

To allow more accuracy in data acquisition, a digital display was used instead of the usual analog systems such as meters or recorders. The trigger from the monostable oscillator mentioned above initiates a pulse in the pulse generator, A, which resets the counter, D, and is delayed 30 ms by an RC network, B, before opening the control flip-flop, C. The signal from the control flip-flop opens gates 1 and 2 and resets the pulse integrator, E. Opening of gates 1 and 2 allows pulses from the clock, D', to start the counter, D. These pulses are integrated in the pulse integrator and the ramp thus generated is compared with the analog input, which has been scaled to a set magnitude by the scaling and polarity amp, G, at the comparator, C. When these two potentials are equal, the comparator closes the control flip-flop, thus stopping the counter and pulse integrator. The scaling and polarity amp circuit is adjusted such that the number displayed on the counter is equal to the current in

the cell for a given gain setting on the polarograph. Thus, these two features of the chronopotentiometer allowed reproducible drop size and reproducible times of current measurement. The current measurements were made as close to the end of the drop as possible to eliminate most of the non-faradaic current. Briefly, the digital display accessory sampled the current input from the polarograph when triggered by the time delay circuit previously mentioned. This potential, which is proportional to the current, was then displayed on a digital counter.

The block diagram in Figure 5 illustrates the operation of the digital display accessory. The counter was a 5216A, 12.5 MHz Counter made by Hewlett-Packard.

Chemicals

Potassium Nitrate

Fisher Chemical Company reagent grade potassium nitrate was used.

Cadmium Nitrate

"Baker Analyzed" reagent grade cadmium nitrate was used.

EGTA

Eastman Organic Chemicals EGTA was used. Solutions 0.01 F in EGTA were prepared for titrations by dissolving the required weight of EGTA and 1.5 equivalents of TMAOH in the appropriate volume of water. The resultant solution was filtered to remove impurities and standardized with a standard cadmium nitrate solution using Eriochrome Black T as the indicator. For polarography 0.01 F solutions of EGTA were prepared as described above except that potassium hydroxide was employed instead of TMAOH.

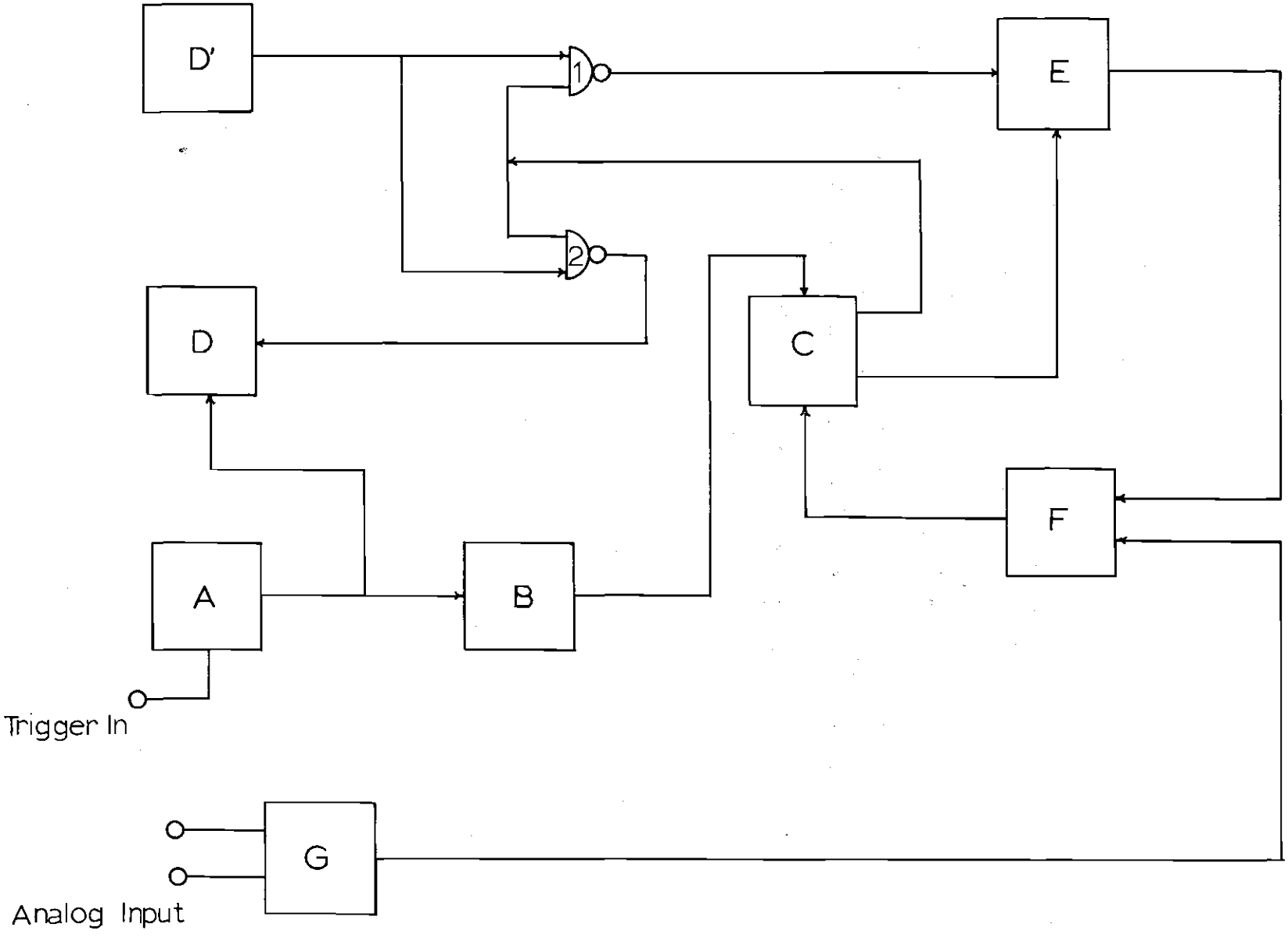

Figure 5. Diagram of the Digital Display Accessory

Potassium Hydroxide

"Baker Analyzed" reagent grade potassium hydroxide was used.

Tetramethylammonium Hydroxide

Eastman Organic Chemicals TMAOH was employed throughout. It was found that the 10 percent solutions that were available had a greater shelf life than the 25 percent solutions that were also purchased. Tests with the ion-selective electrode showed a combined sodium and potassium concentration of 3×10^{-4} F for a 0.1 F solution of TMAOH.

Water

Doubly-deionized water was used for all titrations and polarography work.

Nitrogen

American Cryogenics Company purified dry nitrogen was used for purging all systems.

Mercury

Fisher Chemical Company and Bethlehem reagent grade, triply-distilled mercury was used.

CHAPTER IV

COMPLEXES OF THE CADMIUM-EGTA-POTASSIUM NITRATE SYSTEM

Introduction

In Chapter II it was stated that the formation constants for complexes containing weakly bound metal ions could be studied directly by means of an ion-selective electrode or indirectly in a pH study of the system. For an ion-pair system these same techniques can be applied. With regard to the potassium-EGTA complexes and the ion pairs, it was hoped that the data from the ion-selective electrode on the one hand and from pH titrations on the other would give results that could be cross checked. The pH titrations furnished excellent agreement with the ion-selective electrode in the study of the potassium-EGTA system in the absence of cadmium. There was, however, no significant pH lowering due to the ion pairing of potassium with the complex. The absence of pH lowering effects in the $Cd(EGTA)^{2-}$-KNO_3 system will be discussed later in this chapter.

In order to create a system in which the reduction in potassium ion concentration is essentially due to ion pairing, two restrictions were imposed on the composition of the sample solutions. First, the cadmium concentration was in excess of that of the EGTA. Second, the pH was kept higher than 5.0 to insure that the complexation of EGTA with cadmium was essentially complete. Additionally, operation at pH 5.0 assured that interference in the response of the ion-selective electrode from hydrogen

ion was minimal.

Various methods for use of the ion-selective electrode have been set forward (20) to alleviate such problems as potential drift and variations in the slope of the Nernst plot. These methods were applied to systems that showed only weak complexation and pairing effects. In the present case, however, the ion pairing was present to a much larger extent than expected and the application of a calibration curve obviated all these problems.

A good test for the method used and the electrode response itself was comparison with results from a separate proven method. The work of Watters (15) previously mentioned offered such a method. Thus, potassium complexes of EGTA could be studied with the ion-selective electrode and also by pH-lowering to check the validity of the method in which the ion-selective electrode was employed.

Since the electrochemical phenomena of the cadmium-EGTA system were also to be studied for evidence of ion pairing, a general knowledge of the species present at any given pH was necessary. From the pH titration data of the EGTA-potassium solutions with and without cadmium present, the constants that are necessary to obtain the species distribution were calculated.

Solutions containing cadmium in excess of EGTA were titrated with tetramethylammonium hydroxide in the absence of and in the presence of a potassium nitrate concentration equal to and twice that of EGTA. The variation in potassium nitrate concentration was made in order to check

for any deviations in the ion pair constants due to the formation of a species containing more than one potassium ion. Analogous titrations were performed on solutions which contained no cadmium but were otherwise identical to the above solutions.

Tetramethylammonium hydroxide was used as the titrant in all cases since the tetramethylammonium ion has been reported to be weaker in complexing ability than potassium ion. Subsequent titrations with various amounts of tetramethylammonium chloride present showed that this salt has very little effect, if any, on the pH of a solution at any given point in the titration.

No attempt was made to keep the ionic strength constant. Since the data were to be correlated with those obtained polarographically, the formal concentration of cadmium could not exceed 0.01 F. Thus, the ionic strength of the solutions studied never exceeded 0.05 M and the variation in ionic strength did not exceed 0.01 M. Calculations using the extended Debye-Hückel limiting law showed that variation in the activity coefficient under the above conditions was less than 0.02, which was within the precision of the methods used. Of course, the ionic strengths of the solutions prepared did not agree with those given in connection with acidity constants reported in the literature; therefore, the literature values were not used, but from experimental data new ones were calculated pertaining to the given conditions.

Since the solutions used were a mixture for which Debye-Hückel calculations are less exact than for single salt solutions (21), experimental evidence for activity effects was desired rather than a prediction

of these effects through calculations. Activity effects upon the concentration calibration plots were investigated using the ion-selective electrode. Calibration plots were made from potentiometric data gathered from standard solutions of 0.001 F, 0.006 F, 0.01 F, and 0.02 F potassium nitrate. Each solution was run with tetramethylammonium chloride concentrations of 0.001 F, 0.01 F, and 0.05 F. One set of potentiometric data was obtained from solutions containing no tetramethylammonium chloride. The potentiometric readings and the slopes of the calibration plots for each concentration of tetramethylammonium chloride remained constant within experimental error (± 1 mv).

Calculation of Acidity and Formation Constants

The Use of Bjerrum's Spreading Factor Method

According to Bjerrum (22), the acidity constants of a weak polyprotic acid can be related to the hydrogen ion activity and the ratio of bound protons to acid molecules, $\bar{n}$. This ratio may be expressed by the equation

$$\bar{n} = \frac{C_H - a_{H^+}}{C_{H_sA}} \qquad (4\text{-}1)$$

where

$$C_H = (s - y)C_{H_sA} \qquad (4\text{-}2)$$

with C_{H_sA} being the formal concentration of the acid and y the number of

protons that have been removed from the acid. In alkaline solution, the activity of hydrogen ion is so small that the activity term may be neglected. In acid solution, however, the activity of the hydrogen ion is no longer small enough to be neglected.

EGTA is a tetraprotic acid for which the equations for the dissociation of protons and the respective equations for acidity constants are

$$H_4EGTA \rightleftarrows H_3EGTA^- + H^+ \tag{4-3}$$

$$K_1 = \frac{a_{H^+}[H_3EGTA^-]}{[H_4EGTA]} \tag{4-4}$$

$$H_3EGTA^- \rightleftarrows H_2EGTA^{2-} + H^+ \tag{4-5}$$

$$K_2 = \frac{a_{H^+}[H_2EGTA^{2-}]}{[H_3EGTA^-]} \tag{4-6}$$

$$H_2EGTA^{2-} \rightleftarrows HEGTA^{3-} + H^+ \tag{4-7}$$

$$K_3 = \frac{a_{H^+}[HEGTA^{3-}]}{[H_2EGTA^{2-}]} \tag{4-8}$$

$$HEGTA^{3-} \rightleftarrows EGTA^{4-} + H^+ \tag{4-9}$$

$$K_4 = \frac{a_{H^+}[EGTA^{4-}]}{[HEGTA^{3-}]} \tag{4-10}$$

Since K_2 is so much larger than K_3 (by a factor of 10^6), K_1 and K_2 may be considered independent of K_3 and K_4. Thus, the EGTA system, after neutralization of the first two protons, may be treated as a diprotic acid. To calculate the acidity constants, K_3 and K_4, Bjerrum's case for a diprotic acid is used.

Considering only statistical effects for a diprotic acid, the ratio of the association constants for association of the first proton to association of the second proton should be equal to four. This ratio, however, is dependent upon other effects, also, and is defined as

$$\frac{k_1}{k_2} = 4X^2 \tag{4-11}$$

where X is called the spreading factor and separates the real case from the statistical case.

The relation of $\bar{n}$ to the proton association constants and hydrogen ion activity is

$$\bar{n} = \frac{k_1 a_{H^+} + 2k_1 k_2 a_{H^+}^2}{1 + k_1 a_{H^+} + k_1 k_2 a_{H^+}^2} \tag{4-12}$$

For $\bar{n} = 1$, Equation (4-12) simplifies to

$$k_1 k_2 = \frac{1}{a_{H^+}} \tag{4-13}$$

or

$$\log k_1k_2 = -\log a_{H+} = pH \tag{4-14}$$

Substitution of Equation (4-13) into Equation (4-12) gives

$$\bar{n} = \frac{2X(k_1k_2)^{1/2}a_{H+} + 2k_1k_2a_{H+}^2}{1 + 2X(k_1k_2)^{1/2}\ a_{H+} + k_1k_2a_{H+}^2} \tag{4-15}$$

If $\bar{n}$ is plotted against pH, the slope of $\bar{n} = 1$ will be

$$-0.4343\ \frac{d\bar{n}}{dpH} = \frac{1}{X + 1} \tag{4-16}$$

Rearrangement of (4-11) yields

$$k_1 = 2X(k_1k_2)^{1/2} \tag{4-17}$$

and

$$k_2 = \frac{(k_1k_2)^{1/2}}{2X} \tag{4-18}$$

The association constants may now be calculated. The dissociation or acidity constants are calculated by taking the reciprocal of the corresponding association constants.

Figure 6 exhibits the titration of EGTA with TMAOH. The three curves represent the presence of different concentrations of potassium

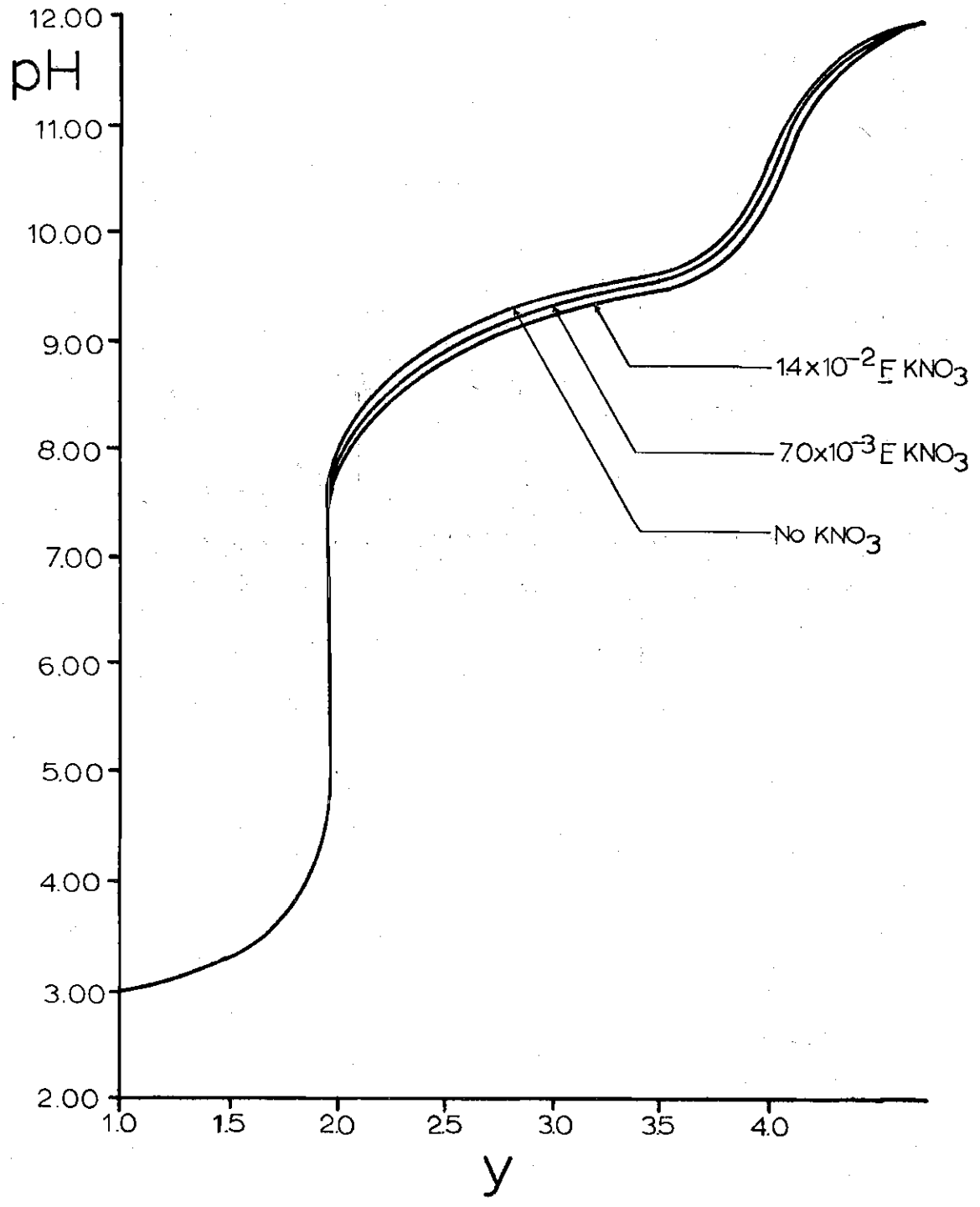

Figure 6. Titration Curves for EGTA with Varying Potassium Nitrate Concentration

nitrate. In each of the curves it can be seen that there are two inflection points--a large one corresponding to the neutralization of the second proton and a small one designating that of the fourth proton.

In the pH region between the two equivalence points, the maximum number of protons on the molecule is two. Thus, it is this system that is studied to calculate constants K_3 and K_4. In solutions containing potassium ion, the constants, K_3 and K_4, are changed in value and are called K_3' and K_4'. The latter constants are dealt with below.

Potassium-EGTA Formation Constants

Equation (2-11) expresses the acidity constant for a solution containing a weak complex and a polyprotic acid. For the potassium-EGTA system

$$K_3' = \frac{a_{H^+}\left([HEGTA^{3-}] + [KHEGTA^{2-}]\right)}{[HEGTA^{3-}]} \qquad (4\text{-}19)$$

and

$$K_4' = \frac{a_{H^+}\left([EGTA^{4-}] + [KEGTA^{3-}]\right)}{[HEGTA^{3-}]} \qquad (4\text{-}20)$$

assuming no bimetal complexes are formed. The equations for the complexing of potassium by EGTA and the respective formation constants are

$$K^+ + HEGTA^{3-} \rightleftarrows KHEGTA^{2-} \qquad (4\text{-}21)$$

$$K_{KHL}^{HL} = \frac{[KHEGTA^{2-}]}{[K^+][HEGTA^{3-}]} \tag{4-22}$$

$$K^+ + EGTA^{4-} \rightleftarrows KEGTA^{3-} \tag{4-23}$$

$$K_{KL}^{L} = \frac{[KEGTA^{3-}]}{[K^+][EGTA^{4-}]} \tag{4-24}$$

where L stands for the ligand EGTA. If Equations (4-22), (4-24), (4-8), and (4-10) are substituted into Equations (4-19) and (4-20), it can be seen that

$$K_3' = K_3 + K_{KHL}^{HL} K_3[K^+] \tag{4-25}$$

and

$$K_4' = \frac{K_4 + K_{KL}^{L} K_4[K^+]}{1 + K_{KHL}^{HL} [K^+]} \tag{4-26}$$

In Figure 6 the results of titrations with varying amounts of potassium nitrate present are shown. At any given amount of TMAOH above pH 7, it can be seen that the pH is lowered with the addition of potassium nitrate.

To calculate the constants K_{KHL}^{HL} and K_{KL}^{L} the acidity constants K_3' and K_4' must first be calculated for the systems containing potassium ion using the spreading factor method. Constants K_3 and K_4 are calculated in the same way for the system containing no potassium ion. For any of

the titrations, values are taken from the pH curve in the range between $\bar{n} = 2$ and $\bar{n} = 0$ and plotted versus pH. The slope is found at $\bar{n} = 1$ and used to calculate the spreading factor via Equation (4-16). Then the spreading factor is employed along with the pH at $\bar{n} = 1$ to calculate the association constants by means of Equations (4-17) and (4-18). The acidity constants are then obtained by taking the reciprocal of the corresponding association constants. It was found that the $\bar{n}$ versus pH plot was a straight line in the range $\bar{n} = 1/2$ to $\bar{n} = 3/2$. Thus the finding of the slope of the plot at $\bar{n} = 1$ posed no problem.

The calculations of K_{KHL}^{HL} and K_{KL}^{L} were done with a computer because the concentration of potassium ion has to be corrected for complexation with the EGTA, a process that requires time consuming reiterations.

The program was based on the idea of a cyclic calculation involving successive approximations. For a single calculation the pH at $\bar{n} = 1/2$, $\bar{n} = 1$, and $\bar{n} = 3/2$ was inputted. The Bjerrum calculation was then made using the slope, $\frac{pH_{3/2} - pH_{1/2}}{1}$, to calculate X. As mentioned earlier, as many as 20 points had been plotted manually and gave the same results as the three point plot. This part of the program calculated the acidity constants. Equations (4-25) and (4-26) were solved for K_{KHL}^{HL} and K_{KL}^{L} respectively and were used to calculate these constants. In the first cycle through this part of the program, the formal concentration of potassium ion was used for calculation of the complexity constants.

To account for the potassium ion which was complexed, a correction had to be made. Equations (4-22) and (4-24) were used to calculate the potassium ion concentration using the values for K_{KHL}^{HL} and K_{KL}^{L} which

were calculated previously in the program. The corrected potassium ion concentration was then applied in the recalculation of the cormation constants. The cycling was continued until the calculated potassium ion concentration was equal to the concentration calculated in the previous cycle. At this point the results were printed out. Fifteen to 20 cycles were generally required for the complete calculation. A print-out of the program is shown in Appendix II.

The results of the pH-lowering method were used to evaluate both the response of the ion-selective electrode in the test solutions, and the method in which this electrode was used. Duplicates of the potassium ion containing samples studied by the pH-lowering technique were employed for the determination of potassium ion using the ion-selective electrode. Since the potassium ion concentration was calculated at $\bar{n} = 1/2$ and $\bar{n} = 3/2$ by the computer program, these concentrations could be compared to those determined with the ion-selective electrode at the corresponding points. Thus, if these values from both methods agreed, it could be said that the calibration-plot method for employing the ion-selective electrode was sufficient for the purposes of this work.

In Table 1 the results of two methods are compared. The close agreement of these results appears to validate the assumption that the methods used were effective. Also, the agreement of these two techniques supports the belief that the values of the constants calculated for the formation of the potassium-EGTA complexes are essentially correct.

Species Distribution of Cadmium-EGTA Complexes

The species distribution for the cadmium-EGTA system is governed

Table 1. Data and Results for the Titration of EGTA in the Presence of Varying Amounts of KNO_3 Using the pH-Lowering Technique and the Ion-Selective Electrode

pH-Lowering Technique

$\bar{n}$	pH	$C_{EGTA} \times 10^3$	$C_K \times 10^3$	$[K^+]_{calc} \times 10^3$	$\log K^L_{KL}$	$\log K^{HL}_{KHL}$
0.50	9.78	6.54	7.46	6.36	1.50 ± .05	
0.50	9.75	6.54	4.8	12.8	1.48 ± .05	
1.50	8.91	6.94	7.75	6.93		1.28 ± .05
1.50	8.88	6.94	15.5	14.1		1.23 ± .05

Ion-Selective Electrode

$\bar{n}$	pH	$C_{EGTA} \times 10^3$	$C_K \times 10^3$	$[K^+]_{obs} \times 10^3$
0.50	9.78	6.54	7.46	6.42
0.50	9.75	6.54	1.48	12.7
1.50	8.91	6.94	7.75	6.90
1.50	8.88	6.94	15.5	14.0

by a number of factors which include pH and the magnitude of the formation constants. Ignoring ion pairing and potassium-EGTA complex formation, the equations for the formation of the several cadmium-EGTA complexes and their respective formation constants are

$$H_2EGTA^{2-} + Cd^{2+} \rightleftarrows Cd(H_2EGTA) \tag{4-27}$$

$$K_{CdH_2L}^{H_2L} = \frac{[Cd(H_2EGTA)]}{[Cd^{2+}][H_2EGTA^{2-}]} \tag{4-28}$$

$$HEGTA^{3-} + Cd^{2+} \rightleftarrows Cd(HEGTA)^{-} \tag{4-29}$$

$$K_{CdHL}^{HL} = \frac{[Cd(HEGTA)^{-}]}{[Cd^{2+}][HEGTA^{3-}]} \tag{4-30}$$

$$EGTA^{4-} + Cd^{2+} \rightleftarrows Cd(EGTA)^{2-} \tag{4-31}$$

$$K_{CdL}^{L} = \frac{[Cd(EGTA)^{2-}]}{[Cd^{2+}][EGTA^{4-}]} \tag{4-32}$$

The acidity constants for the protonated forms are given by

$$Cd(H_2EGTA) \rightleftarrows H^{+} + Cd(HEGTA)^{-} \tag{4-33}$$

$$K_1' = \frac{a_{H^+}\,[Cd(HEGTA)^{-}]}{[Cd(H_2EGTA)]} \tag{4-34}$$

$$Cd(HEGTA)^{-} \rightleftarrows H^{+} + Cd(EGTA)^{2-} \tag{4-35}$$

$$K_2' = \frac{a_{H^+}\,[Cd(EGTA)^{2-}]}{[Cd(HEGTA)^-]} \qquad (4\text{-}36)$$

The calculation of the relative distribution of the various species present at a given pH requires the knowledge of the above formation constants and acidity constants. Since in this study of the relative distribution of the species just a general picture of the system was desired, only the acidity constants K_1' and K_2' were calculated from experimental data. The value for K_{CdL}^{L} was taken from tables listed by Schwarzenbach (23) and the other formation constants, $K_{CdH_2L}^{H_2L}$ and K_{CdHL}^{HL}, were calculated from the derived expressions.

In the cadmium-EGTA system the formal concentration of EGTA may be expressed as

$$C_{EGTA} = [H_4EGTA] + [H_3EGTA^-] + [H_2EGTA^{2-}] \qquad (4\text{-}37)$$

$$+[HEGTA^{3-}] + [EGTA]^{4-} + [Cd(H_2EGTA)]$$

$$+[Cd(HEGTA)^-] + [Cd(EGTA)^{2-}]$$

if the complexes $Cd(H_3EGTA)^+$ and $Cd(H_4EGTA)^+$ are considered to be present in negligible amounts. The concentration of the complex species alone may be expressed as

$$C_{complex} = [Cd(H_2EGTA)] + [Cd(HEGTA)^-] + [Cd(EGTA)^{2-}] \qquad (4\text{-}38)$$

substitution of Equations (4-34) and (4-36) into Equation (4-38) yields

$$C_{complex} = [Cd(H_2EGTA)] + \frac{K_1' [Cd(H_2EGTA)]}{a_{H^+}} + \frac{K_1'K_2' [Cd(H_2EGTA)]}{a_{H^+}^2} \quad (4\text{-}39)$$

The relative distributions of the complex species may now be calculated for any pH.

Calculation of the constants K_1' and K_2' were made using the Bjerrum technique mentioned earlier in this chapter. Solutions used for the study of the acidity constants of the mono- and di-protonated constants consisted of 0.008 F cadmium and 0.007 F EGTA. No complexes of protonation higher than two were assumed to exist. Thus, the situation is that of a weak diprotic acid and allows use of the Bjerrum calculations. In a titration of these solutions the acidity of the protonated complexes will be evidenced physically by a definite slope in the titration curve before the inflection point. In Figure 7 such a titration curve is shown. A comparison of K_2' calculated here with the value of K_2' given by Ringbom (24) suggested that the method was applicable and a correct value had been calculated. Ringbom lists a log value of -3.5 for K_2' while our value was determined to be -3.2. Since the value given by Ringbom was calculated at an ionic strength of 0.1 and the ionic strength of the sample here was approximately 0.02, the difference in constants is reasonable. For K_1' a log value of -2.8 was determined. It was expected that K_1' and K_2' would be of comparable size since the corresponding constants, K_3 and K_4 (pertaining to the unmetallized acid), are almost equal.

In Figure 8 the relative distribution of complex species is shown

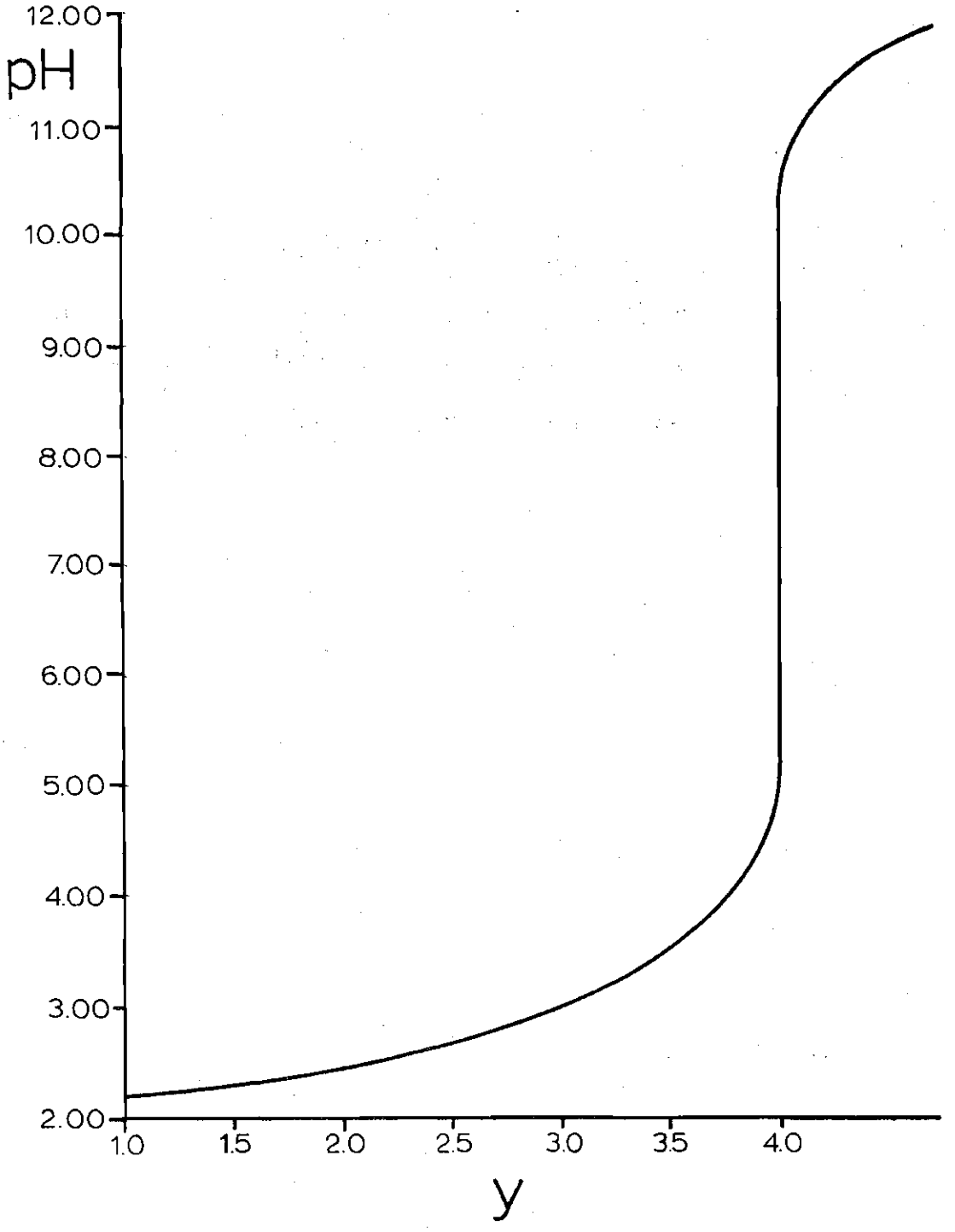

Figure 7. Titration Curve for the Cadmium-EGTA System

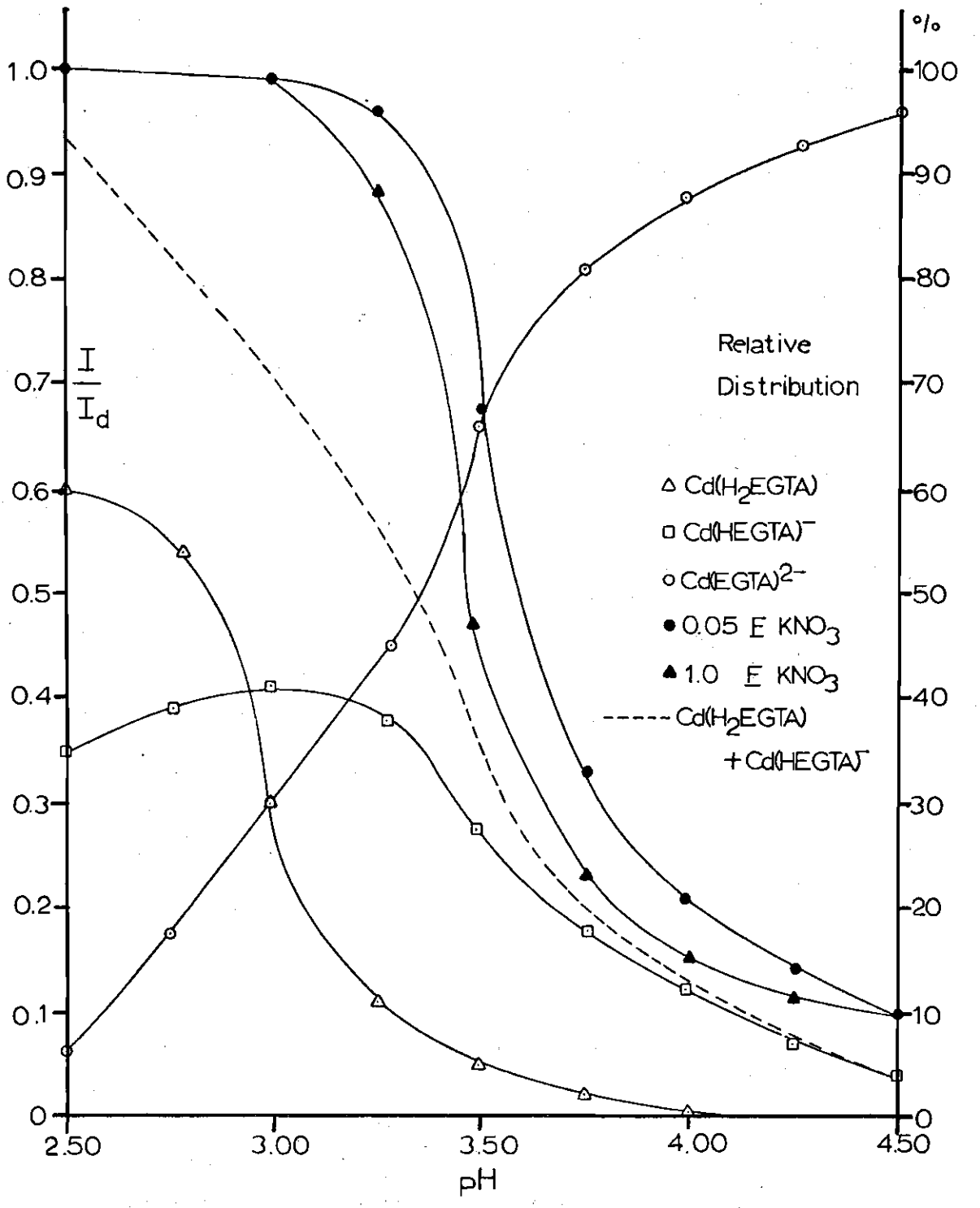

Figure 8. Relation of Species Distribution to Current Lowering

for the range $2.5 \geqq pH \leqq 4.5$. It should be noted that above pH 3.5 the unprotonated complex is the dominant species. Although this series of distribution curves does not show how much of the cadmium is complexed, it does give insight into which species are present at various pH levels.

Cadmium-EGTA-Potassium Ion Pairs

As mentioned earlier, it had been assumed that ion-pair formation would affect the acidity of a protonated cadmium-EGTA complex to an extent sufficient for pH-lowering effects to be observed. Assuming a purely electrostatic type of interaction to be the driving force for ion pair formation, the acidity of a protonated complex $K[Cd(H_xEGTA)]^{(1-x)-}$ should be increased slightly, due to the increased charge on the species. Accordingly, the formation of a bond stronger than in a mixed-metal complex, should increase the acidity even more than it is by the electrostatic interaction. Thus, if pH lowering could be observed, not only the extent of ion pairing could be evaluated, but also hypotheses could be made concerning the type of bonding between the potassium and the EGTA complex. If a mixed-metal type of complex were formed, one would expect pH-lowering effects to be about as great as those due to the potassium-EGTA complex formation; the pH-lowering would occur in the region of the last two equivalence points in the titration of the complex.

In Figure 7 the titration curve for the cadmium-EGTA complex is shown. If Figure 7 is compared to Figure 6 it can be seen that the inflection point in the titration of the cadmium-EGTA complex corresponds to the second inflection point in the titration of the metal-free EGTA. It can also be seen that in Figure 7 no significant pH lowering occurs. The

fact that no pH lowering occurs can be explained in two ways. First, it can be safely said that ion-pair formation, if present, does not enhance the acidity of the protonated cadmium-EGTA complexes to an extent that is measurable with the techniques employed. Thus, since no pH lowering was observed, no indications are present to support the bonding hypotheses. In defense of the method used, one may point out that very strong complexes such as the cadmium-EGTA complex have such an effect on the acid that any effects on pH due to a second weakly bonded metal are unobservable. It is possible that ion-pairing with the protonated complexes of cadmium-EGTA does not exist. This statement, however, is not substantiated by the cation electrode studies presented below or by the polarographic analysis of the system which will be discussed later. Of course, no pH-lowering effects can be seen beyond the inflection point in the titration since all four acid groups are completely neutralized at this point.

Since pH-titration techniques did not show any evidence of ion pair formation, the ion-selective electrode was employed. The experiments to study ion pair formation were performed in essentially the same way as to evidence potassium-EGTA complexation. Due to the sensitivity of the electrode for hydrogen ion, however, no measurements could be made below pH 5. Consequently, measurements were performed in solutions which contained predominantly the $Cd(EGTA)^{2-}$ complex. Thus, it was not possible to determine any ion pairing for protonated cadmium-EGTA complexes. As will be shown later, the extent of ion pairing between potassium ion and the $Cd(EGTA)^{2-}$ species was surprisingly large, a fact that leads to the

assumption that the protonated cadmium-EGTA species is probably also involved in ion pairing.

Solutions were studied which contained varying amounts of potassium nitrate. The EGTA concentration was kept constant and cadmium ion was present in slight excess to prevent errors stemming from excessive formation of potassium-EGTA complexes. Potentiometric measurements were made at various intervals above pH 5. Tetramethylammonium hydroxide was used as the titrant. Interference from the tetramethylammonium ion was minimal (see Chapter III). Calibration plots were made both before and after each run to determine the extent of drift in the ion-selective electrode; however, the drift in potentiometric readings during one run was not noticeable. Over a 24 hour period the drift was 1-2 millivolts.

The equation for the formation of a potassium-$Cd(EGTA)^{2-}$ ion pair and the formation constant are

$$K^+ + Cd(EGTA)^{2-} \rightleftarrows K^+(CdEGTA)^{2-} \tag{4-40}$$

$$K_{KCdL}^{CdL} = \frac{[K(CdEGTA)^-]}{[K^+][Cd(EGTA)^{2-}]} \tag{4-41}$$

Equation (4-41) was used to calculate the formation constant, K_{KCdL}^{CdL}, of the ion pair. The material balance equations in this system for potassium and EGTA, respectively, at pH > 5.0 are

$$C_K = [K^+] + [K(CdEGTA)^-] \tag{4-42}$$

$$C_{EGTA} = [Cd(EGTA)^{2-}] + [K(CdEGTA)^{-}] \qquad (4\text{-}43)$$

Combining Equations (4-41), (4-42), and (4-43) yields

$$K^{CdL}_{KCdL} = \frac{C_K - [K^+]}{[K^+]\left[C_{EGTA} - (C_K - [K^+])\right]} \qquad (4\text{-}44)$$

In Equation (4-44) the possibility of more than one potassium ion paired with the complex is omitted. The intent of this work was to get merely a general picture for the degree of ion pairing; thus, no experiments were run at higher potassium ion concentrations, where such pairing would require consideration.

In Table 2 the results of the ion pairing study via the ion-selective electrode are shown. The relevant data were gathered over a period of three days, and indicate that frequent calibration of the electrode compensates for any drift in its response over long periods of time.

The results of the ion pairing study seem to indicate a slight trend toward larger constants with increasing pH. Whether or not this was due to errors inherent in the electrode was not determined. If, in fact, the trend is existent, the results point to the formation of a mixed metal complex as the driving force in the ion pair formation. Although for the purpose of calculation it was assumed that no protonated complexes exist above pH 5.0, there is a definite probability for the existence of such species in this pH region. This might allow for the fact that the ion pair formation constant seems slightly stronger in the

solutions of higher pH.

It is evident in any case that ion pairing with potassium in the cadmium-EGTA system is present. Surprisingly, the formation constant of the ion pair is about one-half that of the unprotonated potassium-EGTA. This fact leads one to suspect that the bonding of the potassium with the ion pair is of a mixed metal complex type. Since no pH lowering was observed for the system and since the pairing constant was relatively large, too large in fact for a mere electrostatic attraction, it may be concluded that the cadmium has such a large effect upon the EGTA acidity that weakly bound potassium atoms have no measurable effect on the acidity of EGTA.

Table 2. Results of Ion-Pairing Study with the Ion-Selective Electrode

pH	$C_K \times 10^3$	$C_{EGTA} \times 10^3$	$C_{Cd} \times 10^3$	$[K^+]_{obs} \times 10^3$	$\log K_{KML}^{ML}$
5.88	7.46	6.54	7.23	7.03	1.0
6.20	7.46	6.54	7.23	7.20	0.8
9.50	7.41	6.49	7.17	6.85	1.1
9.58	7.41	6.49	7.17	6.90	1.1
5.33	14.9	6.54	7.23	14.0	1.1
5.52	14.9	6.54	7.23	13.9	1.1
9.58	14.8	6.49	7.17	13.6	1.2
9.59	14.8	6.49	7.17	13.5	1.2

CHAPTER V

DETERMINATION OF ELECTROCHEMICAL PARAMETERS

Polarography

The cadmium-EGTA system is not well characterized polarographically. The cadmium-EDTA system, however, has been studied polarographically (26), and results from that work indicate some of the problems to be expected with the present system. Two waves are obtained in polarographic studies of the cadmium-EDTA system. The first of these is well-defined with half-wave potential of - 0.63 and is not pH dependent. This wave is irreversible and is considered to be due to the reduction of the cadmium freed by dissociation of the complex. The second wave is ill-defined and has a pH dependent half-wave potential around -1.2 volts. It is also irreversible and is thought to be due to the direct reduction of complexed cadmium.

The cadmium-EGTA system exhibits similar characteristics. Above pH 2.8, two waves are definitely in evidence and both are irreversible. However, the first wave can be termed quasi-reversible because of its steep slope. Both of the waves are pH dependent as can be seen from the general shapes of the polarograms depicted in Figure 9. Above pH 2.5 the current never reaches the diffusion-limited value that is attained by the aquo-cadmium ion. The decrease in current with increasing pH indicates that complexes are formed which are not reducible at potentials more positive than that for the catalytic reduction of hydrogen ion.

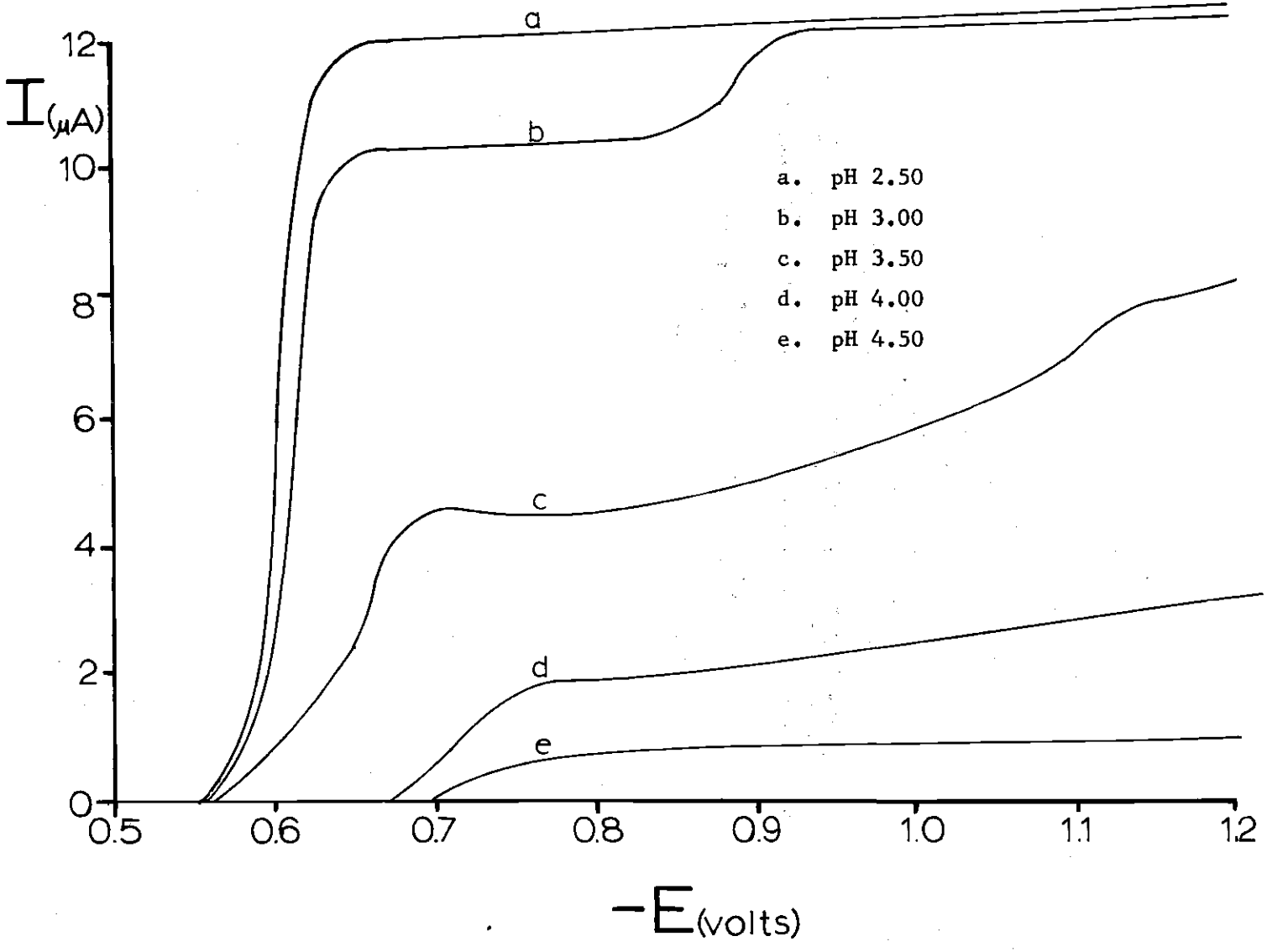

Figure 9. Polarograms for the Cadmium-EGTA System with Varying pH

The ratio of the final currents at various pH to the diffusion current at pH 2.50 gives an indication of the extent of current reduction with an increase in pH. This ratio is shown in relation to the relative distribution of complex species and potassium nitrate concentrations in Figure 8. From this figure it is apparent that the formation of $Cd(EGTA)^{2-}$ is responsible for the reduction of current. It should be noted, however, that the ratio of the total current is higher than the ratio of the concentration of the protonated complexes to the total concentration of all complexes. This fact indicates that the distribution curves plotted do not give an accurate description of the system. Below pH 3.5 there is still some uncomplexed cadmium which gives rise to a current ratio above that predicted by the distribution curves. Above pH 3.5 the distribution curves are probably accurate in describing the system. The discrepancy between the curves at this pH arises because of error in the assumption that no species other than the protonated complexes are reducible. Since the indication is that other species are being reduced, it can be assumed that either $Cd(EGTA)^{2-}$ reacts to a certain minute extent or that an ion pair involving $Cd(EGTA)^{2-}$ is being reduced.

The ratio of the current at the first plateau to the diffusion current is plotted versus pH in relation to species distribution and potassium nitrate concentration in Figure 10. Comparison of Figures 8 and 10 provides some explanations concerning the inaccuracies that were considered above. In Figure 10, as in Figure 8, the currents ratio at pH > 3.5 surpasses the value predicted by the $Cd(H_2EGTA)$-$Cd(HEGTA)^-$ distribution line. In Figure 10, however, at pH > 3.5 this ratio is now about the same as the

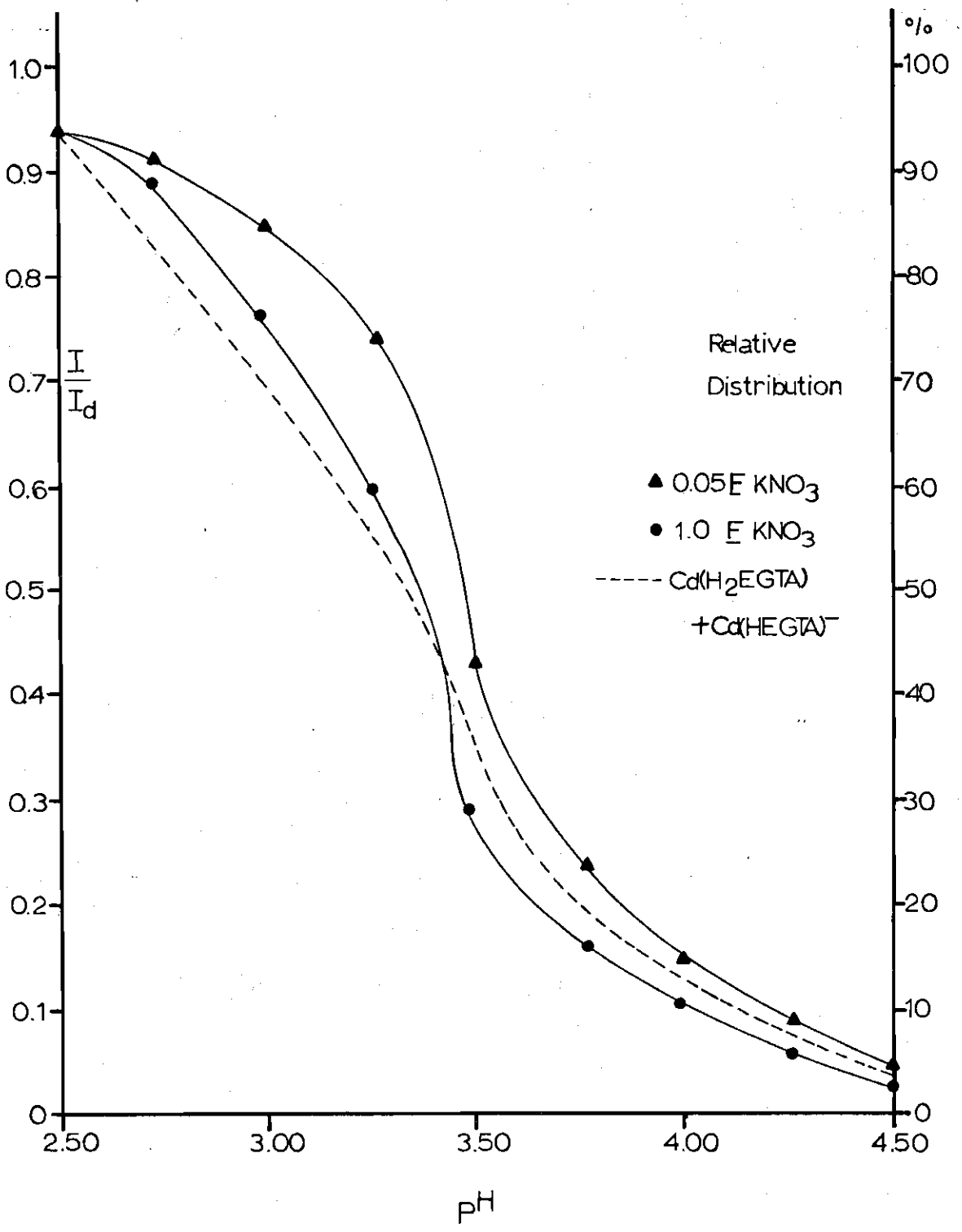

Figure 10. Relation of Species Distribution to Current Lowering in the First Waves of the Cadmium-EGTA System

fraction of protonated complexes. Thus, the $Cd(EGTA)^{2-}$ does not significantly contribute to the current in the first wave.

It should be noted in both cases that increases in the potassium nitrate concentration decrease the current ratios. This is a surprising effect since it is expected that a negative species (i.e. $Cd(HEGTA)^{-}$) would be repelled from the negatively charged electrode and that an increase in the supporting electrolyte concentration should minimize the repulsion and increase the current. If a positive species were being reduced, however, attraction of this species to the electrode is expected due to the effects of the ψ_o potential (see Equation 2-28). In this case, increases in the supporting electrolyte concentration should minimize the attraction and thereby decrease the current. Thus, the decrease in current that is observed with an increase in potassium nitrate concentration can possibly be explained through consideration of a positively charged ion pair.

The two waves exhibited by the system are pH-dependent as can be seen from the data in Table 3. The currents as well as the half-wave potentials are affected by changing the pH. Dependence of the half-wave potential upon pH can indicate not only a change in the species being reduced, but also can point to a different mechanism of electroreduction. Current changes with pH variation indicate a change in the rate of reduction at the electrode, or a change in the reducible species.

Plots of half-wave potentials versus pH are shown in Figure 11. This type of plot, if linear, can give information concerning the number of protons involved in the electrode reaction for a reversible wave.

Table 3. Currents and Half-Wave Potentials for the Cadmium-EGTA System for Varying pH

pH	$C \times 10^3$	$C_{EGTA} \times 10^3$	C_{KNO_3}	$-(E_{1/2})_1$ (v)	$-(E_{1/2})_2$ (v)	i_1 (μA)	i_2 (μA)
2.50	2.04	0	0.1	0.58	---	12.0	12.0
2.50	2.04	4.04	0.1	0.60	---	12.0	12.0
3.00	2.04	4.04	0.1	0.61	0.87	10.2	11.8
3.50	2.04	4.04	0.1	0.65	1.0	4.6	7.2
4.00	2.04	4.04	0.1	0.71	1.1	1.7	2.2
4.50	2.04	4.04	0.1	0.74	> 1.12	0.6	0.8

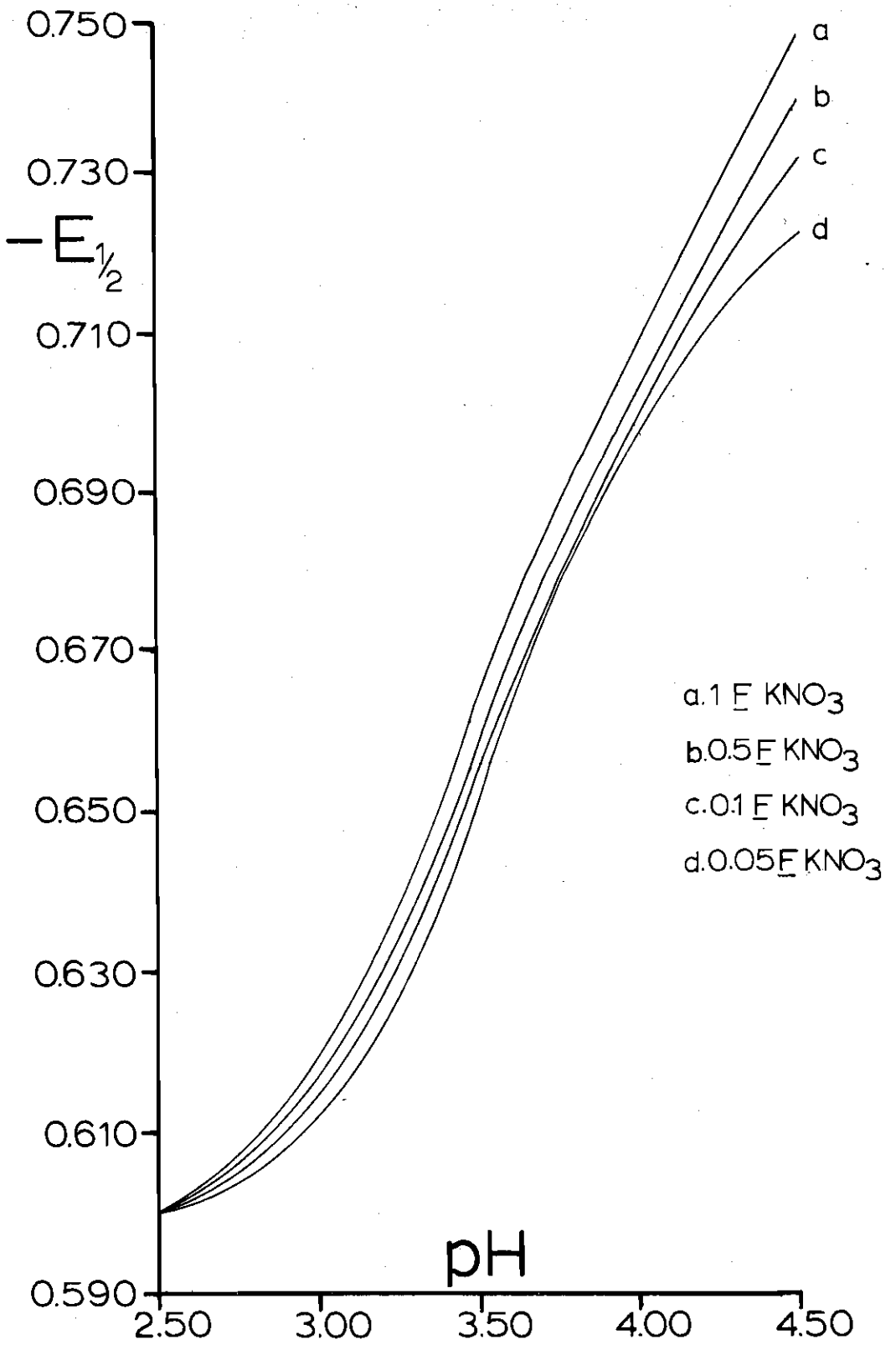

Figure 11. Variation of Half-Wave Potentials with pH

In this case, however, the plots are not linear and the wave is irreversible; therefore, the only conclusion that can be drawn is that, although protons are involved in the electrode reaction, the exact number cannot be determined due to the curvature of the plot. The curvature of the plots is probably due to the fact that more than one species is reducible. It is interesting to note that the potassium nitrate concentration influences the pH effect on the half-wave potential.

Since the aquo-cadmium ion in potassium nitrate has a half-wave potential of about -0.58 volts, all polarographic work with a cadmium system is done on the negative side of the PZC. Previous studies (4) have shown that the effects of potassium nitrate on the double layer are greatest at negative Φ. The above polarographic study, however, only considers half-wave and current phenomena and thus is qualitative with respect to the electrode reaction itself. Effects of the double layer cannot be neglected if a qualitative study of the electrode reaction is to be undertaken. Further studies of double-layer effects are presented below.

Effects of Charge and Specific Adsorption on the Electrical Double Layer Drop-time Curves

In Chapter II it was shown that the charge on the double layer can be related to the interfacial surface tension and that the latter can be related to the drop time of the capillary. By measuring the drop-time of a mercury-filled capillary at a constant head over a range of potentials allows the establishment of the electrocapillary maximum or PZC. The electrocapillary maximum should occur at the potential at which the

interfacial surface tension is at a maximum; therefore, this point corresponds to the maximum drop-time for a given set of conditions.

There are methods for the calculation of the surface tension and the charge from polarographic drop-times (24), but these are inherently of low accuracy. Thus, the information gathered from drop-time-potential curves could only be applied in a general way to look for abnormalities. Literature values, which were obtained by more accurate methods, were available and were used as the basis for double-layer calculations.

Some typical drop-time-potential curves are presented in Figure 12. From such curves it could be determined whether any effects are present which are more significant than those due to potassium nitrate as shown by the data of Payne (4). As evidenced in the curves in Figure 11, no significant surface-activity effects are present. Due to the lack of precision in the method, however, those by themselves do not present evidence to warrant the assumption that no surface-active species are present.

No attempt was made to locate the PZC by means of the drop-time-potential curves, since the apparatus available for the present work was not of sufficient stability to give adequate results. Typical error in the location of the PZC was about $\pm$ 10 mv from one trial to the next.

The important information gained, however, was that no effects were seen with the addition of EGTA and cadmium to the potassium nitrate solutions. Further proof that EGTA and its cadmium complexes are not surface active was obtained from an independent study of the system utilizing double-step chronocoulometry (25). In that work, neither reactants nor reaction products showed a significant degree of specific adsorption. In

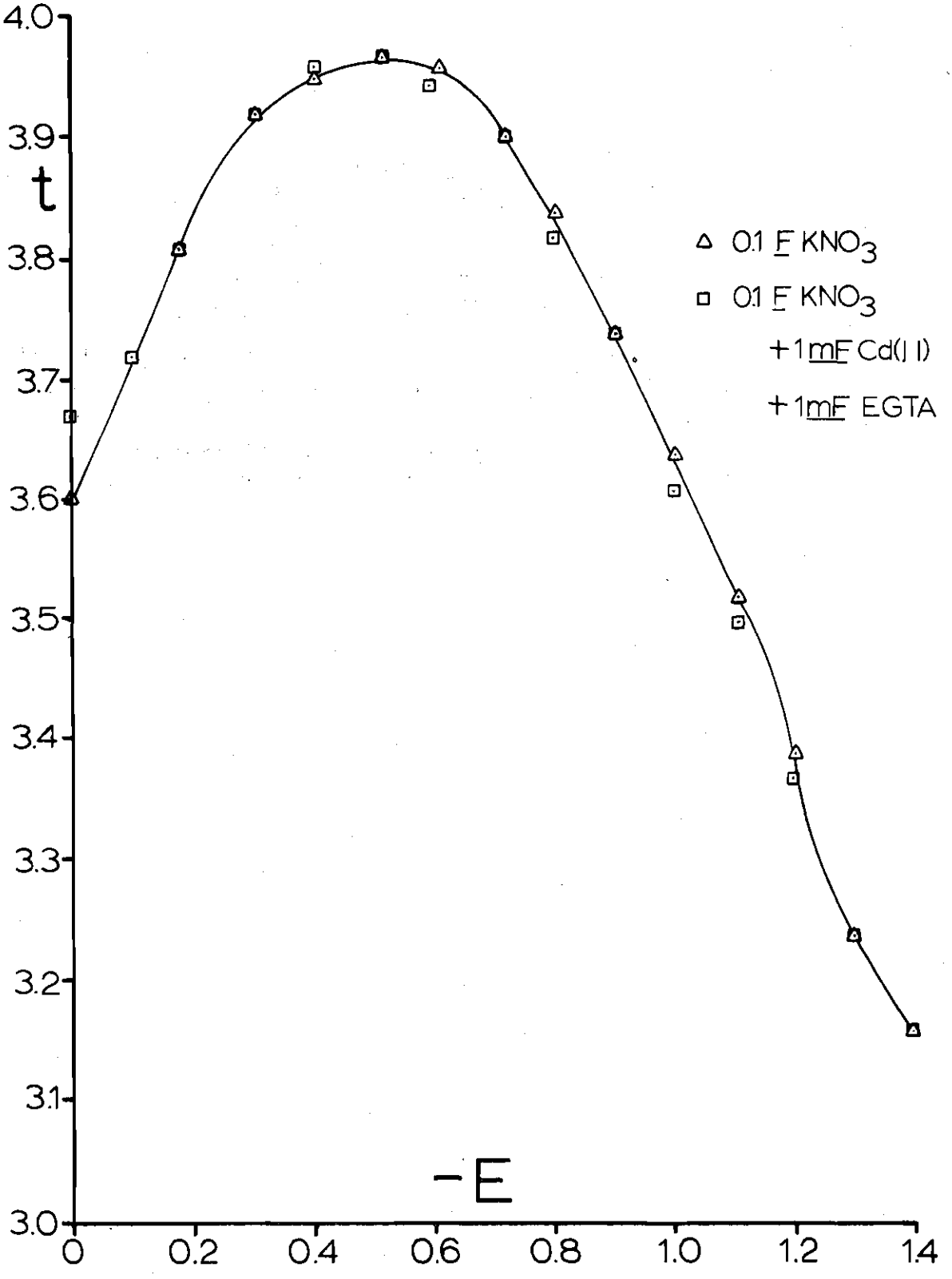

Figure 12. Drop-Time Plots

light of the agreement in the results of the two methods, it was assumed that the addition of cadmium and EGTA in small amounts had very little effect upon the double layer in potassium nitrate solutions of a formality greater than 0.05.

The ψ_o Function

In Chapter II ψ_o was expressed as a function of charge, supporting electrolyte concentration, and surface area of the mercury drop. If these parameters are known and if the supporting electrolyte is of the 1 - 1 variety, ψ_o may be computed from

$$\psi_o = \frac{2}{f} \sinh^{-1} \frac{q}{11.75\ C_s^{1/2}} \qquad (6\text{-}1)$$

Since it was concluded that the charge, q, of the double layer depends only on the potassium nitrate concentration, the comprehensive study of the potassium nitrate system by Payne was used to determine the function ψ_o (4). Figure 13 shows the relation of ψ_o to negative Φ potentials. At $\Phi = 0$ the charge is zero; hence, ψ_o is zero also. This calculation of ψ_o, however, neglects any adsorbed charge, q', and thus is not quite accurate.

Payne lists data relating the charge, q, on the electrode to the adsorbed charge, q', due to adsorption of the nitrate ion on the electrode surface. The latter charge must be taken into account if a more accurate representation of the ψ_o function is to be found. If a new ψ_o function is formulated as

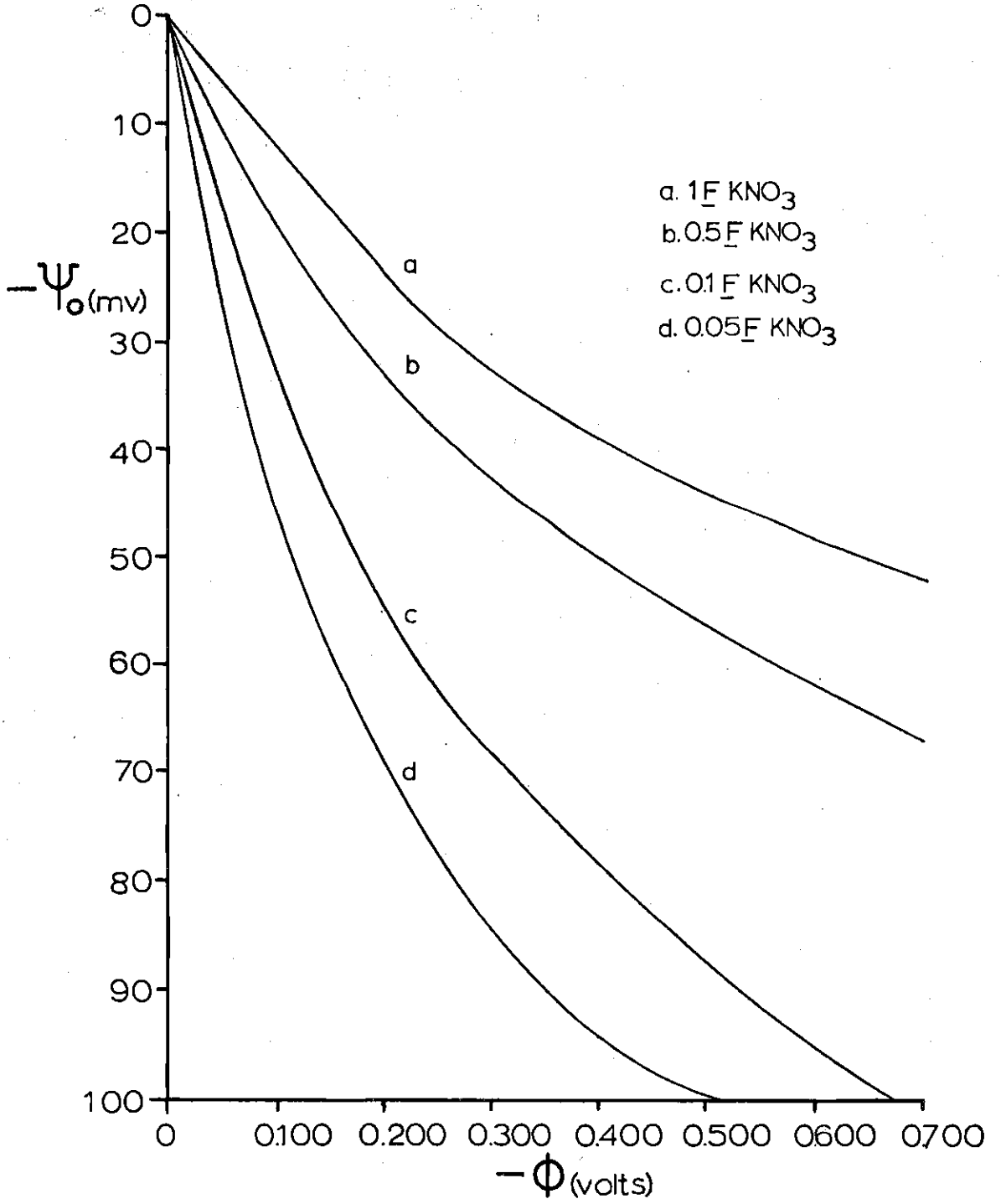

Figure 13. The ψ_o Function Uncompensated for Specific Adsorption

$$\psi_o = F\left[(q + q'),\ C_s\right] \qquad (6\text{-}2)$$

compensation for specifically adsorbed charge can be made.

Using the data of Payne, ψ_o values were calculated for all values of $q + q'$ between 0 and -15 $\mu C/cm^2$. The latter were taken from plots of q' versus q at constant potassium nitrate concentrations of 0.05 F, 0.1 F, 0.5 F, and 1.0 F. Then values for q' versus Φ at constant q were utilized to find q at various values of Φ for the above electrolyte solutions. The function $\psi_o = F\left[(q + q'),\ C_s\right]$ was then plotted versus Φ for the four supporting electrolyte concentrations. These plots are shown in Figure 14.

By comparison of Figures 13 and 14, it can be seen that the specific adsorption of the nitrate affects the potential across the diffuse double layer profoundly. At $\Phi = 0$, if adsorbed charge is taken into account, ψ_o is significantly less than zero. At more negative potentials, however, the differences between the two become less pronounced and at Φ below -0.4 volts, these differences disappear altogether.

It can be concluded that the small adsorption of nitrate on the electrode, if the potential is sufficiently negative, has no effect upon the electrode reaction. However, at potentials close to the PZC adsorption effects are significant. The effect of nitrate adsorption on the rate of the electrode reaction is due only to the resulting change in ψ_o and no physical blocking of the surface is thought to occur. Also, since the reduction of the cadmium-EGTA species occurs at potentials more negative than the PZC, in this case, only the reactions at pH less than 3.5 should be affected by the adsorption of nitrate.

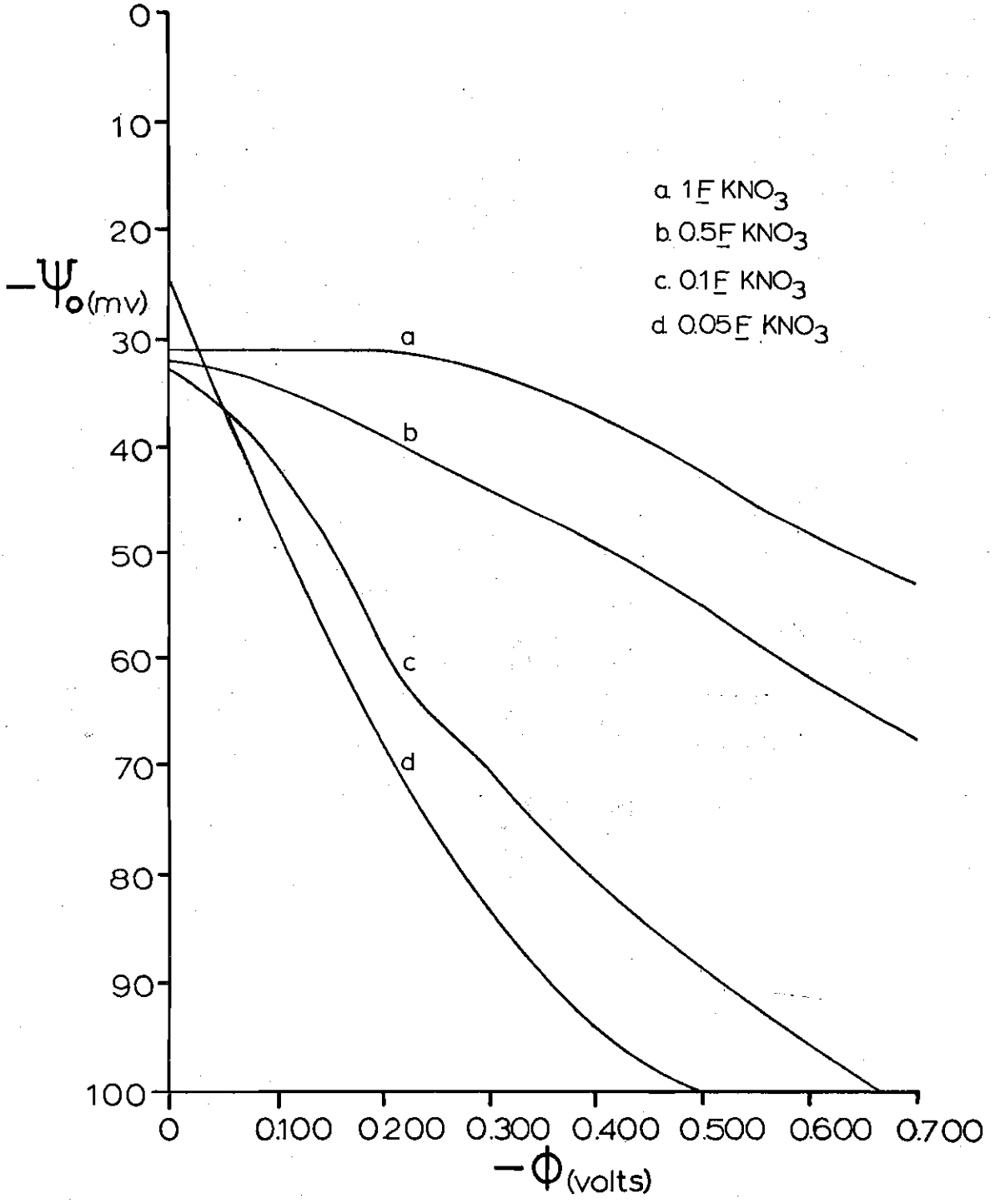

Figure 14. The ψ_o Function Compensated for Specific Adsorption

The Gierst Analysis

Separation of Components of Potential

The rational potential, Φ, is composed of ψ_o, the potential across the diffuse double layer and Φ', the potential across the compact double layer. The driving force of the reaction, Φ', cannot be measured, but ψ_o can be calculated from electrocapillary data and Φ can be measured experimentally. The Gierst method of analysis (3) uses two potentials, ψ_o and Φ', for obtaining electrochemical parameters.

For an electrochemical reaction in which the apparent rate, V*, is a function of both ψ_o and Φ', the Frumkin (19) equation describes the relation between the potentials and V*.

$$V^* = V^o \left[\exp\left(-\alpha n f \Phi'\right)\right] \exp\left(-zf\psi_o\right) \tag{6-3}$$

At 25°C, Equation (6-3) can be rearranged to

$$0.0591 \log V^* = 0.0591 \log V^o - \alpha n \Phi' - z\psi_o \tag{6-4}$$

The apparent rate, V*, was defined empirically in Chapter II as

$$V^* = \frac{1}{1.35}\left[\frac{2x(3 - x)}{5(1 - x)}\right]\left(\frac{D}{t}\right)^{1/2} \tag{6-5}$$

where x is the ratio of measured current to the diffusion current. Since the diffusion-limited current was only reached in solutions of pH 2.5, this diffusion was used in all calculations of V*. A computer pro-

gram developed by Higgins (26), which allowed the calculation of V* as well as calculation of other electrochemical parameters, was used. The print-out of pertinent parts of this program is listed in Appendix III.

From inspection of Equation (6-4) it is evident that graphical presentation will allow the separation of ψ_o and Φ' effects. Thus, a plot of 0.0591 log V* versus ψ_o for constant Φ' will allow z to be found, and a plot of 0.0591 log V* versus Φ' for constant ψ_o will give αn. Once z and αn have been determined, the true rate, V^o, can be calculated.

The actual graphical construction was performed in the following manner. Plots of 0.0591 log V* versus Φ were made from polarographic data from several solutions that differed only in the concentration of the supporting electrolyte. Since the ratio of the concentrations of supporting electrolyte and reducible species was at least 25:1, the structure of the double layer may be assumed to be controlled by the supporting electrolyte. Plots of ψ_o versus Φ for the several supporting electrolytes were made on the same sheet with the $V^* = F(\Phi, C_s)$ plots. The former curves were put at the bottom of the sheet with identical scaling so that no overlap of the curves of the $\psi_o = F(\Phi, C_s)$ and $V^* = F(\Phi, C_s)$ functions occurred (see Figure 15).

Lines were drawn on the $\psi_o = F(\Phi, C_s)$ plot from the points (ψ_o = 0, Φ), at a slope of negative unity, to the Φ axis. Along these lines Φ' is constant. The points of intersection of the constant Φ' lines with the $\psi_o = F(\Phi, C_s)$ curves were then transferred to the $V^* = F(\Phi, C_s)$ curves at the corresponding (Φ, C_s) points. Thus, for any constant Φ' line, there were as many intersections as there were solutions. These points

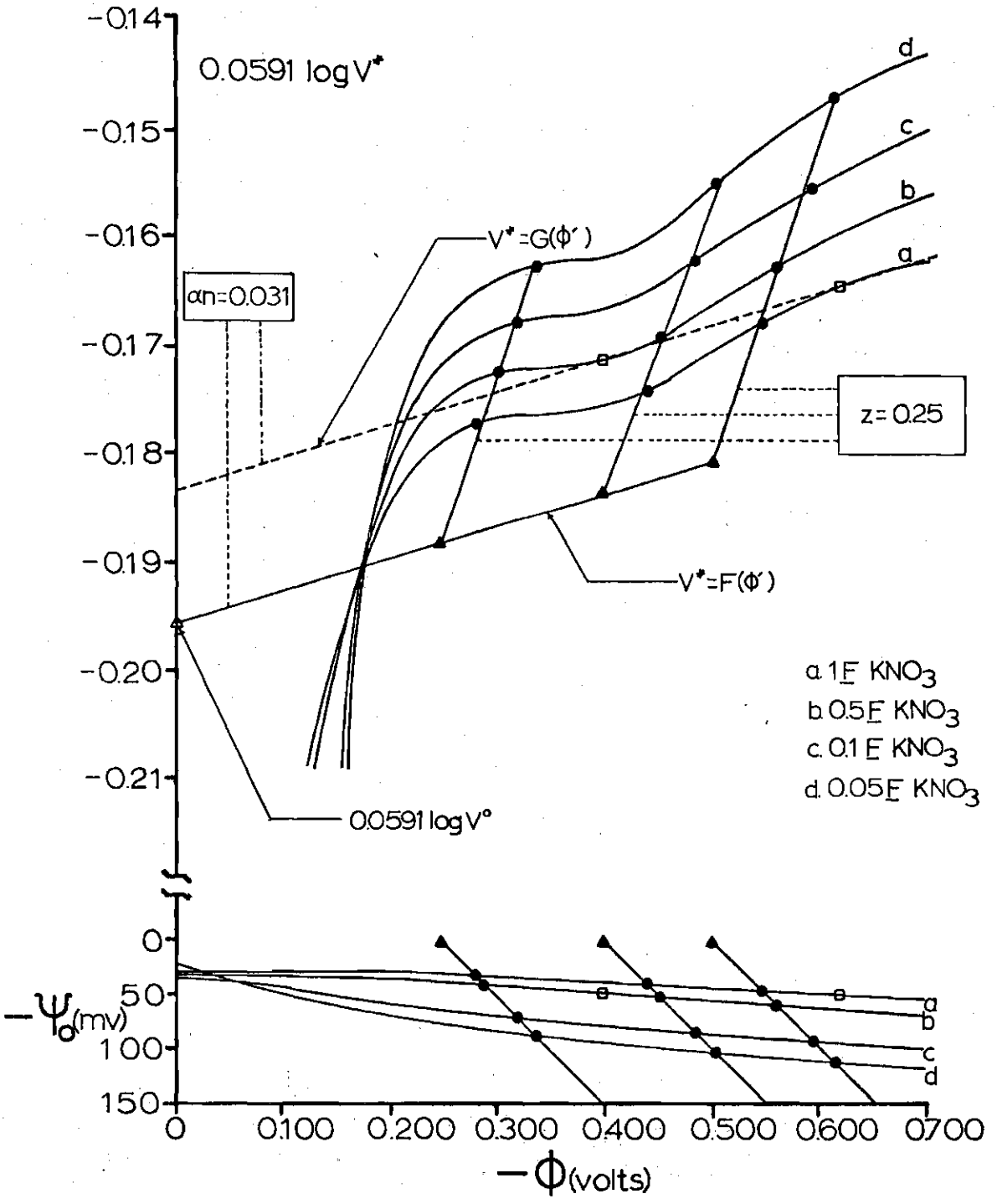

Figure 15. Gierst Plot for Cadmium-EGTA System at pH 3.50

on the $V^* = F(\Phi, C_s)$ curves form a line, $V^* = F(\psi_o)$, with a slope of -z. If the $V^* = F(\psi_o)$ lines are extended to reach the points ($\psi_o = 0$, Φ), these points form another line, $V^* = F(\Phi')$, which has a slope of $-\alpha n$. The intercept of the latter line with the 0.0591 log V^* axis is the point (0.0591 log V^o, $\Phi = 0$) which gives the true rate constant for the electrode reaction in the absence of double-layer effects.

A similar construction was used to check both the data and the method. If points on the $\psi_o = F(\Phi, C_s)$ curves are taken at constant ψ_o and transferred to the corresponding $V^* = F(\Phi, C_s)$ plots, a line, $V^* = G(\Phi')$, is generated which has a slope of $-\alpha n$ and an intercept with the 0.0591 log V^* axis of (0.0591 $V^* - z\psi_o$, $\Phi = 0$).

Although the $V^* = F(\Phi, C_s)$ and $\psi_o = F(\Phi, C_s)$ curves may be drawn on the same graph, it was found that, by having one separate set of $\psi_o = F(\Phi, C_s)$ working curves, the precision of the results of the constructions on the $V^* = F(\Phi, C_s)$ curves was increased.

The Gierst analysis was performed on polarographic data gathered on solutions being 0.05 F, 0.01 F, 0.5 F, and 1.0 F in potassium nitrate. Each solution was run at pH's of 2.50, 3.00, 3.50, 4.00, and 4.50. The pH was adjusted with 1 F potassium hydroxide and/or 1 F nitric acid. All solutions were 2.04×10^{-3} F in cadmium and 4.04×10^{-3} F in EGTA.

The Gierst analysis was initially performed under the assumption that no specific adsorption of the supporting electrolyte is present. The study of Payne, however, showed that specific adsorption of the nitrate ion does occur. Thus, corrections in the value of ψ_o had to be made as shown earlier in this chapter. Corrections in the ψ_o potential were only

significant when operating close to the PZC; however, since the reduction of cadmium-EGTA occurs at more negative values of Φ, compensation of ψ_o for specific adsorption is of questionable use, and only minor changes were noted between corrected and uncorrected plots. All Gierst plots, however, were made using corrected values.

Although at first the value of z was thought by Gierst to be the charge on the electroactive species, Frumkin (19) has shown that it is instead the charge on the species brought to the outer Helmholz plane from the bulk of the solution. In view of the fact that ion-pairing studies by other methods also are concerned with the species in the bulk of the solution, this portion of the Gierst analysis offers an independent look at the same phenomenon.

Results

The Gierst plots for polarograms obtained from solutions of pH 3.50, 4.00, and 4.50 are presented in Figures 15, 16, and 17, respectively. The data for solutions of pH 2.50 and 3.00 will be treated later since the current values for all supporting electrolyte concentrations at both of those pH values were identical within experimental error.

At pH 3.50, a value of 0.25 was determined for z. The slope of both the $V^* = F(\Phi')$ and $V^* = G(\Phi')$ lines was 0.031, showing that a consistent value was found for αn. Extrapolation of the $V^* = F(\psi_o)$ line to $\Phi = 0$ gave a value of 4.9×10^{-4} cm/sec for V^o.

At pH 4.00, the value of z was determined to be 0.19 from the slope of the $V^* = F(\Phi_o)$ lines. Again, both the $V^* = F(\Phi')$ and $V^* = G(\Phi')$ lines gave identical values of αn, but in this case the value was 0.020. V^o was determined to be 1.7×10^{-4} cm/sec.

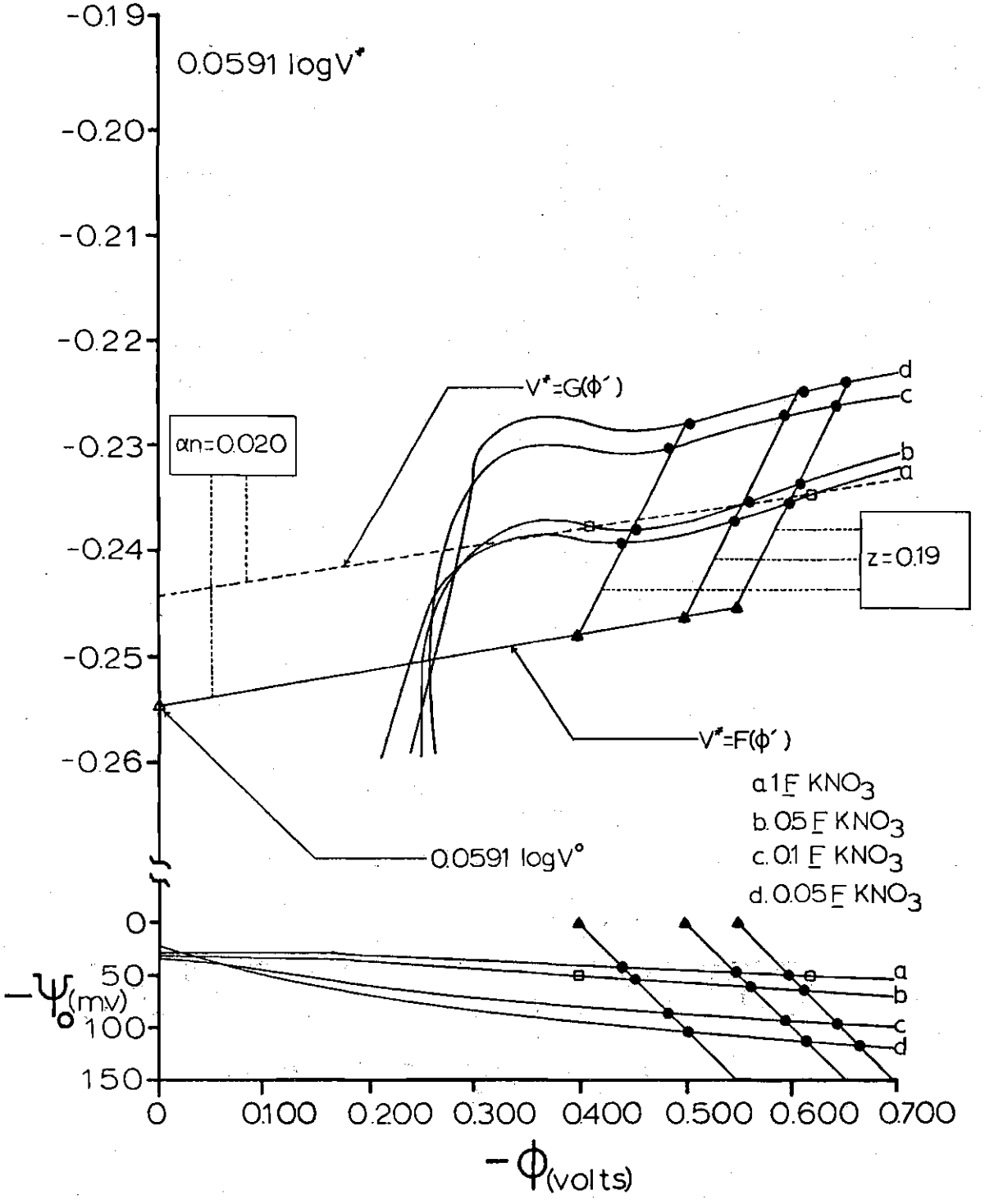

Figure 16. Gierst Plot for Cadmium-EGTA System at pH 4.00

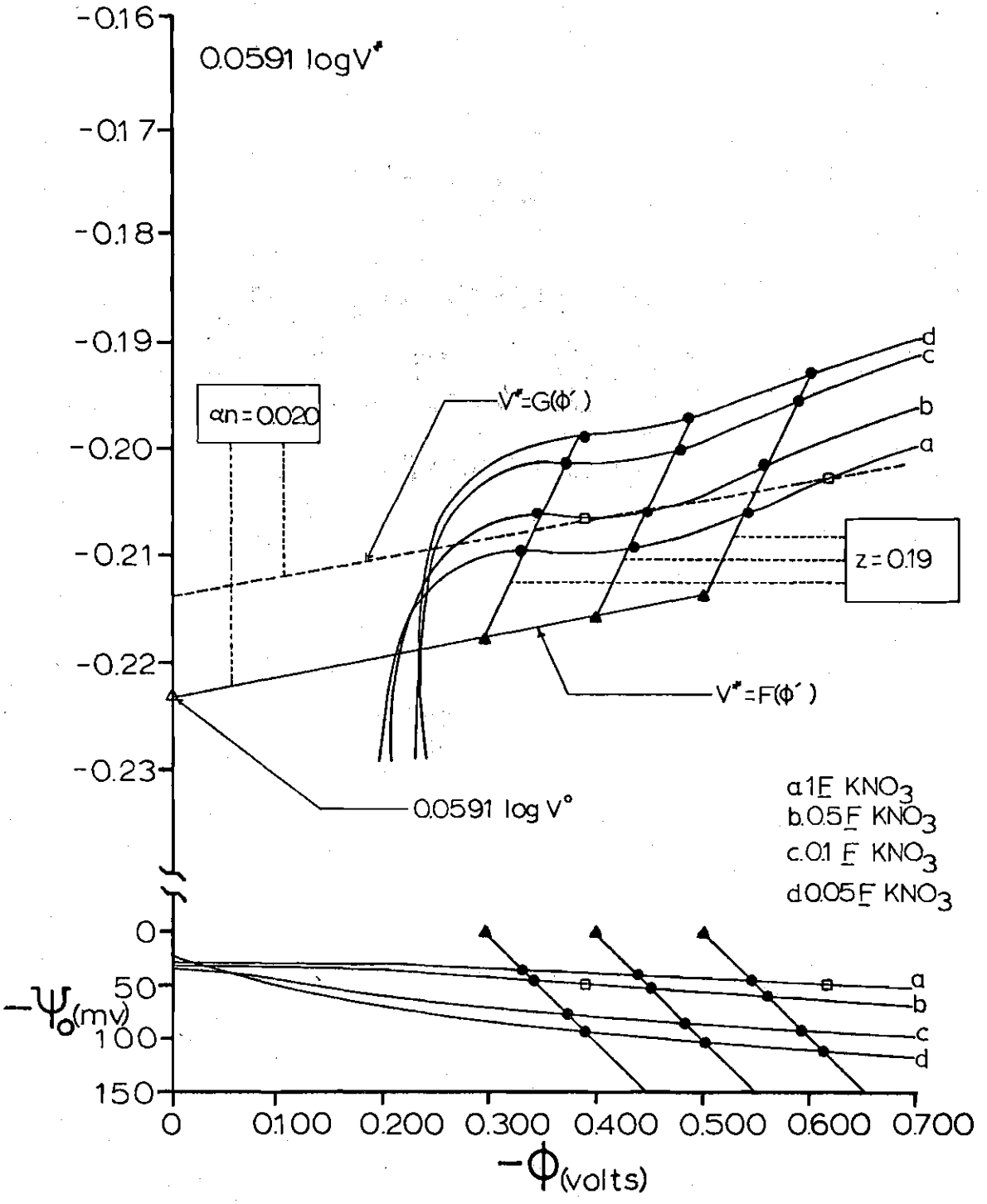

Figure 17. Gierst Plot for Cadmium-EGTA System at pH 4.50

At pH 4.50 the results for z and αn were identical to those at pH 4.00. Agreement was shown between the $V^* = F(\Phi')$ and $V^* = G(\Phi')$ plots. The value of V^o, however, was 5.0×10^{-5} cm/sec.

Discussion

The cadmium-EGTA species are reduced when the electrode is negatively charged. Thus, for a negative species, a repulsion from the electrode is expected in solutions of potassium nitrate concentration below 1 F. The effect of the negatively charged electrode upon a positively charged species is attraction to the electrode. If there is a dependence upon ψ_o, however, the expected concentration of a species at the electrode will be influenced by the ψ_o potential as mentioned earlier in this chapter. The relation between the expected concentration, $[A]^*$, of the electroactive species at the reaction plane to the actual concentration $[A]_o$ is

$$[A]_o = [A]^* \exp(-zf\psi_o) \qquad (6\text{-}6)$$

Thus, for a positive species and a negative ψ_o, the value of $[A]_o$ will increase as Φ becomes more negative, as can be seen in Figures 15, 16, and 17. The value of z was not expected to be positive for the system, but since it was evidenced earlier that the ion-pairing constant was higher than expected, the positive value of z can be rationalized.

Rearrangement of Equation (6-4) and combination with

$$\Phi' = \Phi - \psi_o \qquad (6\text{-}7)$$

results in

$$\psi_o = \frac{0.0591}{\alpha n} \log \frac{V^*}{V^o} + \Phi \left(\frac{1}{1 - \frac{z}{\alpha n}} \right) \qquad (6\text{-}8)$$

If the electrode reaction is a function of ψ_o only, a plot of ψ_o versus Φ at constant V* should result in a straight line of zero slope. A non-zero slope for this line, however, indicates that the electrode reaction is also dependent upon Φ'.

In Figure 18 the plots of ψ_o versus Φ for the several samples are shown. Each plot is for the same value of V*, and values were obtained by drawing lines of constant V* through the steeply rising portions of the $V^* = F(\Phi)$ plots. The abcissa values of the intersects of the constant V* lines gave the values of Φ for one plot and the transposition of each of these values to the corresponding $\psi_o = F(\Phi)$ curve gave a set of corresponding ψ_o values.

The non-zero slopes for the plots in Figure 18 show that V* is not only dependent on ψ_o but also upon Φ'. The changes in slope with pH are an indication that the reacting species is changing, as would be expected.

It is interesting to note that the true rate of the electrode reaction, V^o, changes with pH, even though at pH 4.00 and 4.50 α and z remain constant. The change in V^o is thought to be due to the changes in the distribution of the reacting species when varying the pH. It is not surprising that the rate constant changes even though the reacting species are the same.

Inspection of the Gierst plots in Figures 15, 16, and 17 indicates that, in the range represented by the steeply rising portion, the electrode reaction is more dependent on Φ' than ψ_o.

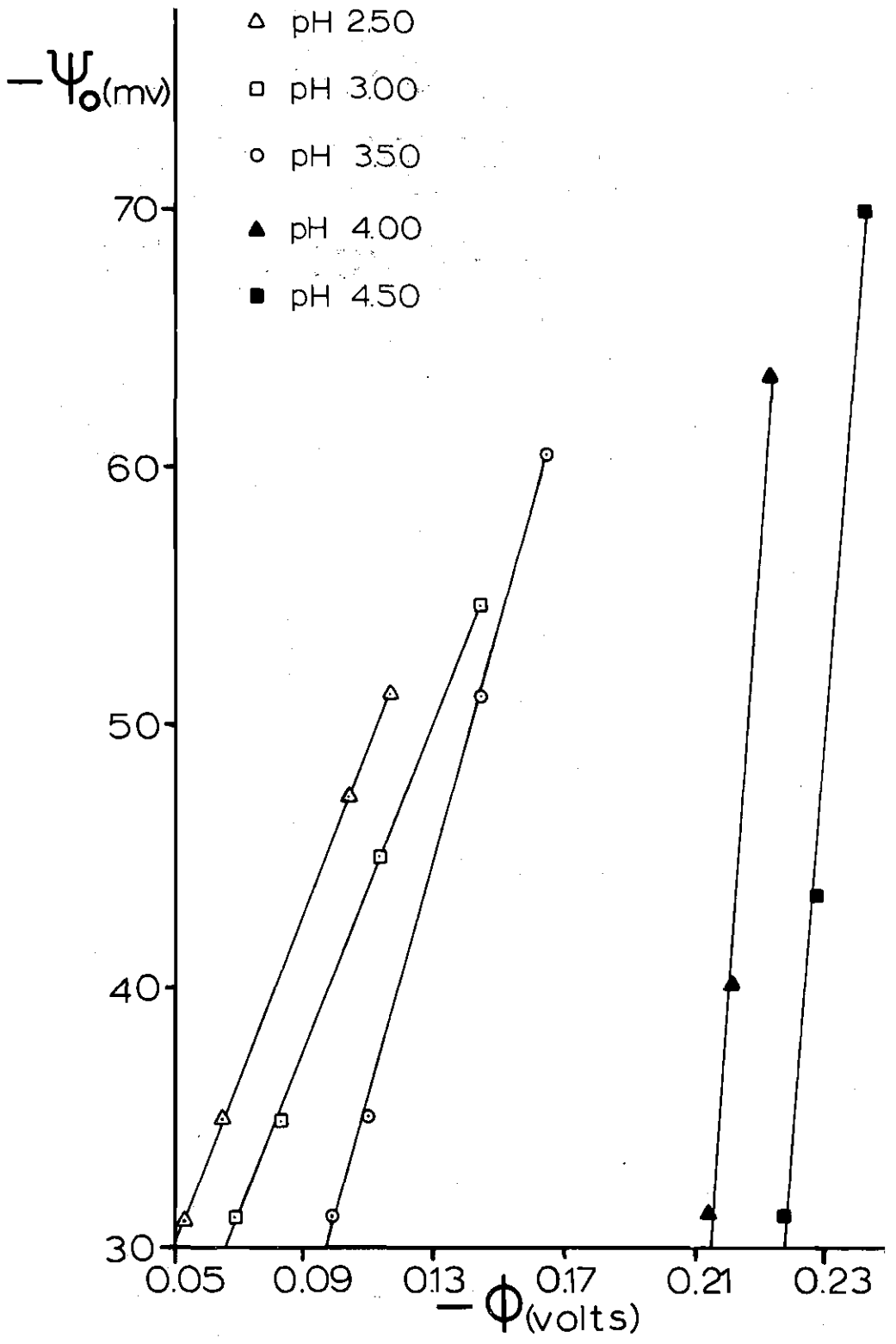

Figure 18. The Relation of ψ_o to Φ at Constant V*

At the crossover point in the plots, the main dependence is on ψ_o as is evidenced by the small variation of V* with Φ. In the rising portion of the curve, the Φ' potential causes the reduction to begin and only at sufficiently negative values of Φ does ψ_o become important enough to halt this rise. For the remainder of the curve, ψ_o is the more significant factor. The dominance of the ψ_o effect is thought to be the cause of the crossover point, since when ψ_o becomes dominant the concentration of reducible species at the electrode surface is influenced greatly.

The value of α, if n is assumed to be 2.0, is quite small. In other work (27), faradaic rectification studies resulted in the calculation of 0.12 for α in a 10^{-3} F cadmium nitrate solution. The supporting electrolyte in that work was 1.0 F potassium nitrate. Even though no truly valid comparison between values of α for the cadmium-EGTA system and an uncomplexed cadmium system can be made, it may be assumed that α is small. It must be remembered that the α value for the cadmium-EGTA is of necessity a composite value, depending on the reduction of at least three different species. Also, the uncomplexed cadmium ion is reduced reversibly, whereas the cadmium-EGTA complex species are reduced irreversibly.

Ion pairing is evidenced in this system by the positive values of z. From the distribution curves in Chapter IV, it is evident that, in the pH range studied, no cadmium-EGTA species exists that carries a positive charge. Also, above pH 3.50, essentially all the cadmium may be assumed to be complexed. The values of z cannot be explained, however, without the assumption that more than one potassium ion is associated

with a cadmium-EGTA complex ion. The formation of complexes such as $K_2Cd(HEGTA)^+$ and $K_2Cd(EGTA)$ was not considered in other studies of the system, but it is apparent that the probability for their existence is high.

Dissociation of the various cadmium-EGTA complexes is not thought to contribute to the high value of z, since any uncomplexed cadmium brought to the electrode would be reduced at the normal half-wave potential for free cadmium and dissociation of the complex in the double layer would not have any effect on the value of z obtained by this method.

Conclusions

The direct determination of ion pairing given in Chapter IV gave results which showed that an ion pairing constant of 10 could be calculated for the formation of a $K(CdEGTA)^-$ species. Since that work considered the formation of only one paired species due to the restrictions that had to be put on the solution for proper response of the ion-selective electrode, assumptions concerning additional ion pairs could only be conjectured. In this work, the concentration of potassium was only twice that of all complex forms so that pairing beyond the mono-potassium form would be difficult to see.

From the results of the study of the electrochemical parameters presented in this chapter, it is evident that a high degree of ion pairing exists in the system. In polarographic work the solutions contained up to 250 times the concentration of potassium ion as was used in the ion-selective electrode study. Thus, it is not unreasonable to expect additional ion pairs to be formed and to be of significant concentration.

The positive value of z obtained from the Gierst plots can only mean that ion pairs such as $K_2(CdHEGTA)^+$ and $K_2(CdEGTA)$ are extensively present at pH 4.00 and 4.50 and that $K(CdH_2EGTA)^+$ is present at pH 3.50.

It can be concluded from this study that ion pairing of potassium with cadmium complexes of EGTA is a phenomenon not only of the electrode double layer but also of the bulk of the solution. The extent of ion pairing in the bulk of the solution is comparable to that of potassium-EGTA complexation. Additionally, studies at the electrode show that ion-pair formation is even more extensive in solutions of high potassium concentration. Possibly, the high degree of pairing shown at the electrode is due not only to the high concentration of potassium in the bulk but also is due to the even higher concentration of potassium at the reaction plane when the electrode is negatively charged.

Sources of Error

Uncertainty arises in any graphical analysis from the drawing of the best line through a set of points. Thus, the values for αn and z could be in error by as much as 10 percent. The value of V^o is even more sensitive to this type of error since it is found from an extrapolation and is determined as a logarithmic function.

The diffusion coefficient used in all cases was that calculated by rearrangement of the Ilkovic equation. The diffusion coefficient was then calculated by substitution of values for diffusion current, mercury flow rate, and the time elapsed at the instant of current measurement into the rearranged equation. The diffusion current was that of a solution 2.04×10^{-3} F in cadmium, 4.04×10^{-3} F in EGTA, and 1.0 F in potassium

nitrate. The value for the flow rate was calculated as described in Chapter III and the measurement of instantaneous current was 3.00 seconds after the fall of the previous drop. A value of 2.87×10^{-5} cm^2/sec was obtained for the diffusion coefficient and employed in all other calculations. Although this diffusion coefficient was necessarily a composite function, it was believed that variations from this value, if any, were small. This value was considered more accurate than one which could be calculated at higher pH values where a diffusion-limited current was not obtained.

The precision of polarographic data was ± 1.0 mv for potentials and ± 0.02 μA for currents as is usual with d.c. polarography. There was no correction made for the internal resistance (i.e. that across the double layer), although the external cell resistance (i.e. the IR drop across the bulk of the solution) was compensated for with the potentiostat circuit described in Chapter III. Corrections for background current were made via an empirical equation in the computer program developed by Higgins (26). The results obtained with this equation agreed well with those from graphical compensation for background current.

APPENDICES

APPENDIX I

LIST OF SYMBOLS AND ABBREVIATIONS

Latin

a	an activity
A	the electrode surface area
C	formal concentration
C_d	the differential capacitance
C_i	the integral capacitance
D	a diffusion coefficient
E	a potential
f	the ratio $\frac{F}{RT}$
F	Faraday's constant
k	the heterogeneous rate constant at a given potential (Chapter II)
k	an association constant (Chapter IV)
k_a^s	the standard apparent heterogeneous rate constant
K	an acidity constant
n	the number of electrons involved in an electrochemical reaction
P	permeability ratio
q	the charge density, $\frac{Q}{A}$
Q	the charge on the electrode
R	the gas constant
t	time

Latin

T	absolute temperature
U	mobility ratio
V	potential (volts)
V*	the heterogeneous rate constant
V^{o}	the true heterogeneous rate constant corrected for double-layer effects
x	the ratio of current to diffusion limited current
z	the charge on any species

Greek

α	the cathodic transfer coefficient
γ	the interfacial surface tension
ϵ	the dielectric constant
Φ	the rational potential
Φ'	the potential across the compact double layer
ψ_o	the potential across the diffuse double layer

Units of Measure

cm	centimeters
cm^2	square centimeters
ml	milliliters
ms	milliseconds
mv	millivolts
sec	seconds
μA	microamperes
μC	microcoulombs

APPENDIX II

WIPL PROGRAM FOR THE CALCULATION OF POTASSIUM-EGTA FORMATION CONSTANTS

```
1.01 COMMENT THIS PROGRAM IS NAMED KEOCALC
1.1 DECLARE K1[100], K2[100]
1.2 DECLARE KK[10], K3[10], K4[10]
1.3 Y=0
1.4 ACCEPT Z
1.5 ACCEPT PH12. H22, PH32
1.6 Y=Y+1

2.1 KK[Y]=(1.00000)/H22
2.2 DEL=(0.4343)/(PH12-PH32)
2.3 X=(1-DEL)/(DEL)
2.4 K4[Y]=(1.0000)/(2*X*KK[Y])
2.5 K3[Y]=(2*X)/(KK[Y])
2.55 PRINT FORM 2.56, Y,KK[Y], K3[Y], K4[Y]
2.56 FORM Y=&  KK=@@@@@@@@@@@@  K3=@@@@@@@@@@@@  K4=@@@@@@@@@@@@
2.57 GO TO 2.6
2.6 IF(Y-Z)1.5, 3.01

3.01 Y=1
3.03 ACCEPT K1[1], K2[1]
3.04 N=1
3.1 KMHL=0
3.15 KML=0
3.3 KMHL=(K3[Y+1]-K3[1])/(K3[1]*K1[N])
3.4 KML=(K4[Y+1]*(1+K2[N]*KMHL)-K4[1])/(K4[1]*K2[N])
3.5 N=N+1
3.6 K1[N]=(-1.0000+SORT(1+4*KMHL*K1[1]))/(2*KMHL)
3.7 K2[N]=(-1.0000+SORT(1+4*K2[1]*KML))/(2*KML)

4.1 IF(K1[N]-K1[N-1])3.1, 5.1, 5.1
4.2 IF(K2[N]-K2[N-1])3.1, 5.1, 5.1
4.4 SET KML=LOG10(KML)
4.5 SET KMHL=LOG10(KMHL)

5.1 PRINT FORM 5.2, N, K1[N], K2[N], LOG10(KML), LOG10(KMHL)
5.2 FORM N=&& K1=@@@@@@@@@@@@ K2=@@@@@@@@@@@@ KML=&&.&&& KMHL=&&.&&&
5.3 PRINT FORM 5.4, KML, KMHL
5.4 FORM          KML=&&.&&&              KMHL=&&.&&&
5.5 Y=Y+1
5.6 IF(Y-Z)3.03, 5.7
5.7 STOP
```

APPENDIX III

FORTRAN PROGRAM FOR THE CALCULATION OF ELECTROCHEMICAL PARAMETERS

```
C
C   BEGIN TO READ DATA SET OF SEVERAL POLAROGRAMS
C
      READ (1,23) TDATE
   23 FORMAT (8A4)
  100 DO 9 I=1,100
    9 MSPACE(I)=1
      READ (1,33) TITLE
   33 FORMAT (20A4)
      READ (1,30) TLIST,IGRAPH,MLIST,MGRAPH,MGCT,MGCH
   30 FORMAT (6(9X,I1))
      MC1=1
      M=0
C
C   READ DATA SET OF A SINGLE POLAROGRAM  108-101
C
  108 M=M+1
      READ (1,11) ID(M),ES(M),CM(M),CL(M),PH(M),FLM(M),T(M),XN,HHG(M)

   11 FORMAT (I5,F10.0,2E10.0,5F9.0)

      IF (ID(M).EQ.0) GO TO 450
      IF (ID(M).EQ.10000) GO TO 501
      IF (ID(M).EQ.20000) GO TO 502
   10 DO 101 J=1,36,5
      LL=0
      JJ=J+4
      READ (1,12) ID(M),(CURRAW(K),E(K),K=J,JJ)
   12 FORMAT (I5,5(2F7.0,1X))
      IF (ID(M)) 500,400,400
  400 DO 102 K=J,JJ
      IF (CURRAW(K))102,103,102
  102 CONTINUE
  101 CONTINUE
      STOP
C
C   END OF ONE POLAROGRAM
C   FOLLOWING STEPS, IN ORDER, CORRECT FRR BACKGROUND (D) 104), TEST TO
C     WHETHER REVERSE REACTION IS NEGLIGIBLE, AND DISCARD POINTS TOO CLO
C     LIMITING CURRENT AND CALCULATE LIMITING CURRENT (D) 114)
C
```

```
  103 L=K-1
      DO 104 I=1,L
      CUR(I)=ABS(CURRAW(I)-(-0.02-0.111*E(I)-0.02*E(I)**3))
      Z(I)=EXP((XN*38.935)*(E(I)-ES(M)))
  104 CONTINUE
      CURD=CUR(L)
      DIFCUR = 0
      LC = 1
      LD = 0
      DO 114 I=1,L
      IF (Z(I)-ZTEST) 112,112,111
  111 LC = I
  112 IF (CUR(I)-(0.99*CURD)) 114,114,113
  113 DIFCUR = DIFCUR + CUR(I)
      LD = LD+1
  114 CONTINUE
      DFCURT(M)=DIFCUR/FLOAT(LD)
      D(M)=(DFCURT(M)/(706.*1000.*XN*CM(M)*(FLM(M)**R23)*(T(M)**R16)))**
     1 2
      DO 105 I=1,L
      IF (CUR(I)-0.98*DFCURT(M)) 110,109,109
  109 IF (LL) 500,300,110
  300 LL=I-1
      LB=I
  110 X(I) = CUR(I)/DFCURT(M)
  105 CONTINUE
      DO 200 I=1,LL
      Y(I)=ALGO10(ABS (((2.*X(I))*(3.-X(I)))/(5.*(1.-X(I))))  )
  200 CONTINUE
      IM=1+(M-1)*50
      DO 201 I=1,50
      WRITE(10) IM,E(I),CUR(I),X(I)
      IM=IM+3
  201 CONTINUE
C
C   REGRESSION ANALYSIS, IRREVERSIBLE THEORY
C
      CALL SOMFIT  (E,Y,LC,LL,W,B,C,SE2,SE,SY,SYE,SY2)
      WC(M)=W*1.

      ALPHA(M)=ABS((0.0592*B)/XN)
      EHALF(M)=(-C/B)
      IF (0.1-EHALF(M)+ES(M)) 117,116,116
  116 XKS(M)=(1./1.35)*((D(M)/T(M))**0.5)*EXP((EHALF(M)-ES(M))*ALPHA(M)*
     1 XN*38.935)
                                                                      S
                                                                  START OF

      GO TO 118
  117 XKS(M)=0.0
  118 DO 107 I=1,LL
```

```
      VSTAR(I)=((8.*X(I)*(3.-X(I)))/(27.*(1.-X(I))))*((D(M)/T(M))**0.5)
      FVSTAR (I) = (1./38.935)*  ALOG (VSTAR(I))
      YREV(I) = ALOG10 (X(I)/(1-X(I)))
  107 CONTINUE
      VTWO=(((SY2)-(SY**2/W))-(B**2)*((SE2)-(SE**2)/W))/(W-2)
      VB(M)=ABS(VTWO/(SE2-((SE**2)/W)))
      VXO=(ABS(VTWO/(B**2))*(1.+(1./W)+((SY/W)**2)/((B**2)*(SE2-
     1 ((SE**2)/W)))))
      VEHF(M)=ABS(VXO)
      I=W-2
      IF (I.GT.32) I=32
      YINTCP=ST(I)*VXO**0.5
      EHALFR(M)=2.*YINTCP
      EHALFS=EHALF(M)+YINTCP
      EHALFT=EHALF(M)-YINTCP
      YTLT=ST(I)*(ABS(VTWO)**0.5)/((SE2-((SE**2)/W))**0.5)
      YSLP(M)=B
      YSLPR(M)=2.*YTLT
      YSLPS=YSLP(M)+YTLT
      YSLPT=YSLP(M)-YTLT
      DO 250 I=LC,LL
      YFIT(I) =SY/W+B*(E(I)-(SE/W))
      DELTAY(I) = YFIT(I)-Y(I)
  250 CONTINUE

      SUBROUTINE SOMFIT (E,Y,LC,LL,W,B,C,SE2,SE,SY,SYE,SY2)
      DIMENSION E(50),Y(50)
      INTEGER W
      SE2=0.0
      SE=0.0
      SY=0.0
      SYE=0.0
      SY2=0.0
      W=LL=LC+1
      IF (W-2) 119,120,121
  119 LC=LC-2
      GO TO 122
  120 LC=LC-1
  122 W=LL-LC+1
  121 DO 106 I=LC,LL
      SE2=SE2+E(I)**2
      SE=SE+E(I)
      SY=SY+Y(I)
      SYE=SYE+Y(I)*E(I)
      SY2 = SY2 + Y(I)**2
  106 CONTINUE
      C=(SYE*SE-SY*SE2)/(SE**2-(W*SE2))
      B=(W*SYE-SE*SY    )/((W*SE2)-(SE**2))
      RETURN
      END
```

APPENDIX IV

FORTRAN PROGRAM FOR THE CALCULATION OF ψ_o

```
C       THIS PROGRAM CALCULATES PSI(0) FROM THE THEORETICAL CONSIDERATIONS

        DIMENSION PSI(10,300),Q(10,300),C(100)
        Z=0
        J=1
        JJ=J+6
        READ(5,100) (C(K),K=J,JJ)
  100   FORMAT (7(F10.0))
        DO 104 Z=1,JJ
        C(Z)=C(Z)**.5
        DO 103 Y=1,300
        Q(Z,Y)=.1*(Y=150)
        X=Q(Z,Y)/(11.74*C(Z))
        PSI(Z,Y)=(2/38.935)*ALOG(X+(X**2+1)**.5)
  103   CONTINUE
  104   CONTINUE
        Z=0
        K=1
        DO 107
        PRINT 105
  105   FORMAT ("0                    C                PSI                Q")
        C(Z)=C(Z)**2
        DO 108 Y=1,300
        PRINT 106, C(K), PSI(Z,Y), Q(Z,Y)
  106   FORMAT (20X, F5.2, 14X, F7.4, 14X, F6.2)
  108   CONTINUE
        K=K+1
  107   CONTINUE
        STOP
        END
```

LITERATURE CITED*

1. Gibson W. Higgins and P. E. Sturrock, Anal. Chem., 41, 633(1969).

2. R. W. Schmid and C. N. Reilley, J. Am. Chem. Soc., 80, 2101(1958).

3. L. Gierst, "Transactions of the Symposium on Electrode Processes," E. Yeager, Editor, John Wiley and Sons, New York, 1961, pp. 109-138.

4. R. Payne, J. Electrochem. Soc., 113, 999(1966).

5. P. Delahay, "Double Layer and Electrode Kinetics," Interscience, New York, 1965, p. 33.

6. F. Haber and Z. Klemensiewicz, Z. Physic. Chem., (Leipzig), 67, 385(1909).

7. W. S. Hughes, J. Am. Chem. Soc., 44, 2860(1922).

8. K. Horovitz, Z. Physic., 15, 309(1923).

9. G. Eisenman, "Advances in Analytical Chemistry and Instrumentation," Vol. 4, C. N. Reilley, Ed., Interscience, New York, 1965.

10. Ibid., pp. 225-228.

11. Ibid., p. 216.

12. Ibid., p. 217.

13. Ibid., p. 308.

14. A. E. Martell and G. Schwarzenbach, Helv. Chim. Acta, 39, 653 (1956).

15. J. I. Watters, S. M. Lambert, and E. D. Loughran, J. Am. Chem. Soc., 79, 3651(1957).

16. K. B. Oldham and E. B. Parry, Anal. Chem., 40, 65(1968).

*Journal title abbreviations used are listed in "Index of Periodicals," Chemical Abstracts, 1970.

LITERATURE CITED (Concluded)

17. P. Delahay, "Double Layer and Electrode Kinetics," Interscience, New York, 1965, p.21.

18. Ibid., p. 29.

19. A. N. Frumkin, O. A. Petry, and Nicolaeva-Fedorovich, Electrochim. Acta, 8, 177(1963).

20. William D. Anstine, M.S. Thesis, Ga. Inst. of Tech., Atlanta, Ga., 1969.

21. G. A. Rechnitz and S. B. Zamochnick, Talanta, 11, 1061 (1964).

22. H. A. Laitinen, "Chemical Analysis," McGraw-Hill, New York, 1960, pp. 10-13.

23. J. Bjerrum, "Metal Ammine Formation in Aqueous Solution," P. Haase and Sons, Copenhagen, 1941.

24. G. Schwarzenbach and H. Flaschka, "Complexometric Titrations," Methuen and Co. LTD., London, 1969, p. 11.

25. A. Ringbom, "Complexation in Analytical Chemistry," Interscience, New York, 1963, p. 334.

26. R. G. Barradas and R. M. Kimmenle, Can. J. Chem., 45, 109(1967).

27. J. A. Liddle, unpublished work, May, 1971.

28. Gibson W. Higgins, private communication, April 1971.

29. G. C. Barker, Trans. Symp. Electrode Proc., Philadelphia, 1959, Wiley, New York, 1961, p. 325.

VITA

Walter McDonald Shackelford was born to Walter Malcolm and Mamye Felder Shackelford on January 8, 1945, in Birmingham, Alabama. He attended public schools in the states of Mississippi and Georgia and graduated from LaGrange High School, LaGrange, Georgia, in June, 1963. He attended the University of Mississippi and graduated with a Bachelor of Science degree in chemistry from that institution in June, 1967.

In September, 1967, he entered the Graduate Division of the Georgia Institute of Technology in the School of Chemistry and was granted a National Defense Education Act Fellowship. In September, 1970, he was appointed a teaching assistant.

In August, 1970, he married Bonnie Ann Freeman.